JOURNAL OF GEOPHYSICAL RESEARCH, VOL. 102, NO. B6, PAGES 12,061–12,084, JUNE 10, 1997

Southeast Pacific tectonic evolution from early Oligocene to Present

S. F. Tebbens

Department of Marine Science, University of South Florida, St. Petersburg

S. C. Cande

Scripps Institution of Oceanography, La Jolla, California

Abstract. Plate tectonic reconstructions of the Nazca, Antarctic, and Pacific plates are presented from late Oligocene to Present. These reconstructions document major plate boundary reorganizations in the southeast Pacific at chrons 6C (24 Ma), 6(o) (20 Ma), and 5A (12 Ma) and a smaller reorganization at chron 3(o) (5 Ma). During the chron 6(o) reorganization it appears that a ridge propagated into crust north of the northernmost Pacific-Antarctic Ridge, between the Chiloe fracture zone (FZ) of the Chile ridge and Agassiz FZ of the Pacific-Nazca ridge, which resulted in a northward jump of the Pacific-Antarctic-Nazca (PAC-ANT-NAZ) mid-ocean triple junction. During the chron 5A reorganization the Chile ridge propagated northward from the Valdivia FZ system to the Challenger FZ, through lithosphere formed roughly 5 Myr earlier at the Pacific-Nazca ridge. During this reorganization a short-lived microplate (the Friday microplate) existed at the PAC-ANT-NAZ triple junction. The PAC-ANT-NAZ triple junction jumped northward 500 km as a result of this reorganization, from a location along the Valdivia FZ to a location along the Challenger FZ. The chron 5A reorganization also included a change in spreading direction of the Chile and Pacific-Antarctic ridges. The reorganization at chron 3(o) initiated the formation of the Juan Fernandez and Easter microplates along the East Pacific rise. The manner of plate boundary reorganization at chron 6(o) and chron 5A (and possibly today at the Juan Fernandez microplate) included a sequence of rift propagation, transfer of lithosphere from one plate to another, microplate formation, and microplate abandonment and resulted in northward migration of the PAC-ANT-NAZ triple junction. The associated microplate differs from previously studied microplates in that there is no failed ridge.

Introduction

Over the past 25 Myr, the southeast Pacific (Plate 1) is known to have undergone many plate boundary reorganizations and triple junction migrations. Such triple junction migrations have been assumed to occur as long periods of steady migration interrupted by occasional "jumps" in location relative to plate boundaries. The mechanism and cause of these jumps remained vague or unknown. A companion paper [*Tebbens et al.*, this issue] found that at chron 5A there was a major plate boundary reorganization and that an accompanying triple junction migration was accomplished by rift propagation, microplate formation, and microplate extinction. In that case, both ridge axes of the Friday microplate continued spreading as "captured" segments of the Chile Ridge and Pacific-Antarctic Ridge. In this paper we demonstrate that this process of "stepwise triple junction migration" apparently also occurred at chron 6(o), between troughs A and B, and may now be occurring at the Juan Fernandez microplate.

The southeast Pacific is currently composed of three major plates: the Pacific (PAC), Antarctic (ANT), and Nazca (NAZ) plates (Plate 1) [*Herron*, 1972]. The NAZ plate is a fragment of the former Farallon (FAR) plate. The first use of marine magnetic anomalies to interpret spreading rate history was at the PAC-ANT ridge at the dawn of the plate tectonic revolution [*Pitman and Heirtzler*, 1966]. Additional data have enabled an improved understanding of the evolution of the southeast Pacific [*Morgan et al.*, 1969; *Herron*, 1971, 1972]. In particular, work in the 1970s found early evidence for plate boundary reorganizations at chron 6C [*Handschumacher*, 1976] and chron 5A [*Weissel et al.*, 1977] based on observed changes in magnetic anomaly and fracture zone (FZ) trends in the vicinity of the Selkirk trough [*Handschumacher*, 1976; *Weissel et al.*, 1977]. We will demonstrate that the Selkirk trough formed during the chron 6C reorganization as the pseudofault of a propagating ridge with no resulting change in triple junction location. The Crusoe trough, a newly identified trough west of the Selkirk trough, formed as the pseudofault of a propagating ridge during the chron 5A reorganization, which resulted in a stepwise triple junction migration [*Tebbens et al.*, this issue]. A more recent study of the evolution of the southeast Pacific by *Mayes et al.* [1990], which included two reconstructions since chron 21 (47 Ma) (at chron 7 (25 Ma) and chron 3(o) (5 Ma)) did not constrain the timing and manner of plate boundary reorganizations, which are the focus of this work.

An improved understanding of southeast Pacific tectonic evolution is now possible due to new geophysical data, in particular, additional magnetics data along the Chile ridge

Paper number 96JB02582.
0148-0227/97/96JB-02582$09.00

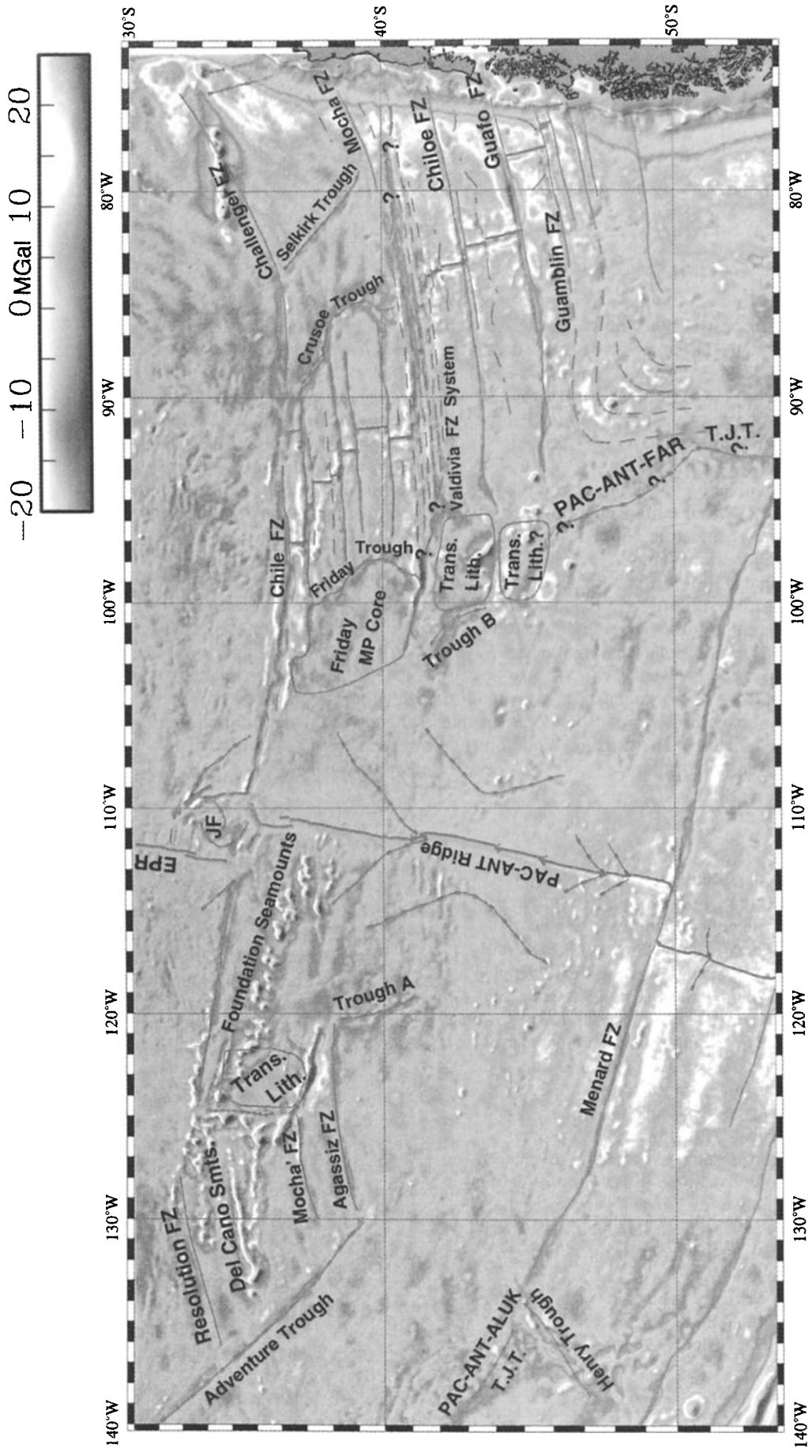

Plate 1. Satellite-derived gravity field of the southeast Pacific [*Sandwell*, 1993] overlain by major tectonic features including ridge axes (heavy solid lines), fracture zones (FZs) (solid and dashed lines, well-constrained and poorly constrained, respectively), nontransform offsets (dash-dotted lines), triple junction traces (dashed lines with dots) and other tectonic discontinuities including pseudofaults, and ridge jumps (solid lines with dots). We have adopted and/or modified previous tectonic interpretations, as stated in text.

[*Tebbens et al.*, this issue] and the high-resolution Geosat geodetic mission satellite altimetry data [*Sandwell and Smith*, 1995]. This paper builds upon earlier observations from the Chile ridge and its flanks and complements the tectonic history of the northeast Pacific of *Mammerickx and Klitgord* [1982], *Atwater* [1989], and *Lonsdale* [1991].

Stepwise Triple Junction Migration Model

Northward jumps in the location of the PAC-ANT-NAZ triple junction occurred at chrons 5A [*Tebbens et al.*, this issue] and 6(o). At chron 5A the method of triple junction migration was accomplished by ridge propagation, microplate formation, and microplate extinction [*Tebbens et al.*, this issue]. We propose that this is a recurring process in the southeast Pacific. We will outline this process using the Juan Fernandez microplate as an example. The nomenclature of *Hey et al.* [1977], *Hey et al.* [1980] and *Naar* [1992], including overlapped ridge and failed ridge, is used to discuss the features associated with propagating rifts and microplates. This stepwise triple junction migration model incorporates the current understanding of processes at present-day microplates [*Hey et al.*, 1985; *Engeln et al.*, 1988; *Searle et al.*, 1989; *Naar and Hey*, 1991; *Larson et al.*, 1992; *Naar*, 1992], with the exception that it does not consider rotation [*Larson et al.*, 1992; *Schouten et al.*, 1993; *Searle et al.*, 1993; *Rusby and Searle*, 1995]. The data associated with extinct microplates along the PAC-ANT-NAZ triple junction path are insufficient to resolve whether or not extensive rotation (>30°) occurred, as is observed at the Juan Fernandez and Easter microplates (78° and 88°, respectively, according to *Searle et al.* [1993]).

First, we consider how a microplate forms. For the Juan Fernandez microplate, some details of formation remain unknown. Microplate formation from an overlapping spreading center has been observed at the Easter microplate [*Searle et al.*, 1993, and references therein], and this same process could have resulted in the creation of the Juan Fernandez microplate, as modeled by *Larson et al.* [1992]. Alternatively, the Juan Fernandez microplate may have formed by a large-offset propagating rift which initiated along the northernmost transform fault of the Chile ridge [*Bird and Naar*, 1994] (Figure 1, Chron 3). Microplate formation by large-offset rift propagation at chron 5A (the Friday microplate) is supported by our reconstructions. By either mechanism, once the microplate has formed, rift propagation occurs as the microplate grows (e.g., the eastern rifts of the Easter, Juan Fernandez, and Friday microplates).

During rift propagation, the propagating ridge and overlapped ridge both spread independently, at different rates and perhaps in different directions, from the major ridge axes. A microplate develops between the propagating ridge and overlapped ridge (Figure 1, present geometry). Before microplate formation, there were three plates and a single triple junction. While the microplate exists, there are three triple junctions, one between each of the three plate pairs and the microplate [e.g., *Larson et al.*, 1992].

Second, how does the microplate become extinct and what are the significant consequences? *Larson et al.* [1992] noted that if the Juan Fernandez microplate were to become attached to the ANT plate, the microplate would become extinct and the PAC-ANT-NAZ triple junction would migrate to the northern microplate boundary (Figure 1, future geometry). The west and east ridge axes of the Juan Fernandez microplate would continue spreading and become the northernmost PAC-ANT ridge and northernmost Chile ridge, respectively. A single PAC-ANT-NAZ triple junction would then be located at the northern boundary of the extinct microplate. This process we call "stepwise triple junction migration" [*Tebbens et al.*, this issue]. Through microplate formation and extinction, the triple junction would have jumped northward. The data indicate that this evolutionary mechanism (i.e., stepwise triple junction migration) also occurred at the Friday microplate.

Larson et al. [1992] also noted that failure of either the east

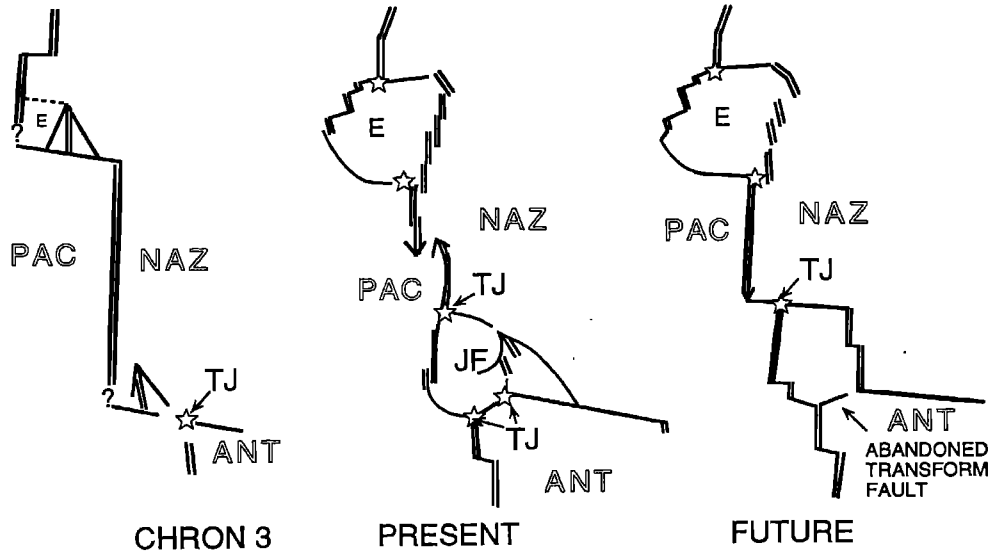

Figure 1. Model of tectonic evolution of the Juan Fernandez microplate. The possible future evolution results in microplate extinction with no failed ridge and a stepwise triple junction migration. Triple junctions (open stars), ridge axes (double lines), transform faults, and psuedofaults (single lines, dashed where tentative) are shown. "JF" is Juan Fernandez microplate, "TJ" is triple junction. See text for discussion.

or west ridge of the microplate is possible and could result in microplate extinction. This evolution would not result in stepwise triple junction migration.

There is a significant difference in the fate of the microplate ridge axes between evolutionary models of microplates which involve stepwise triple junction migration, as proposed above for the Juan Fernandez microplate (Figure 1), and those which do not. For microplates that form and die without resulting in stepwise triple junction migration, such as the Mathematician microplate [*Mammerickx et al.*, 1988] and the Bauer microplate [*Lonsdale*, 1989b], the demise of the microplate occurs when one microplate ridge axis ceases spreading and becomes a fossil ridge axis. In the case of microplate evolution which results in a stepwise triple junction migration (e.g., Friday microplate), both ridge axes of the microplate are captured by the major ridge axes and continue spreading. There are no fossil ridge axis or failed rift features typical of microplate extinctions that do not result in stepwise triple junction migration.

Mammerickx et al. [1988] define an extinct microplate, which they call a paleoplate, as a microplate where dual spreading (i.e., east and west microplate rifts) has ceased and full spreading has resumed at the prevailing spreading ridge. We propose to broaden this definition such that an extinct microplate is a microplate where dual spreading at rates and directions independent of the major axes has ceased and either one ridge has failed and one has continued spreading ("prevailed") or both ridge axes have been captured as segments of major active ridge systems.

Repeated midocean triple junction migration in the stepwise manner described above (Figure 1) will result in a trail of paleoplates marking the triple junction path. Such a trail is observed in the ANT plate from 36°S to ~44°S (Plate 1). The boundaries between paleoplates correspond with the latitudes of FZs formed at the Chile ridge.

Data

Magnetic anomaly, FZ, pseudofault, and fossil ridge axis locations in the southeast Pacific were digitized for use in reconstructions. For crust formed at the Chile Ridge the tectonic maps of *Tebbens et al.* [this issue] were used. For crust formed at the PAC-ANT ridge, the PAC-ANT ridge axis and propagators of *Lonsdale* [1994] and magnetic anomaly picks of *Molnar et al.* [1975] were adopted. *Mammerickx's* [1992] recent interpretation of the crust between the Resolution and Agassiz FZs, in the vicinity of the Foundation seamounts, including a region of transferred lithosphere, was adopted. We modified *Mammerickx's* [1992] interpretation, with (1) a change in the name of the Del Cano FZ to Del Cano seamounts, as explained below; and (2) the addition of the Mocha' FZ, which is evident as a linear low in the gravity field at 37°S (Figure 1). The interpretation of the Adventure trough on the PAC plate is after *Cande and Haxby* [1991], the Henry trough on the PAC plate is after *Cande et al.* [1982], and the Juan Fernandez microplate is after *Larson et al.* [1992].

FZs near 130°W on the PAC plate at roughly 33°S and 40°S have previously been given multiple names in the literature. We follow the nomenclature of *Cande and Haxby* [1991], *Cande et al.* [1989] and *Mammerickx* [1992] in that the FZ at 33°S is the Resolution FZ and the FZ at 40°S is the Agassiz FZ.

A new pair of features have been charted, troughs A and B, flanking the PAC-ANT ridge in roughly chron 6(o) crust. Trough A is on the PAC plate south of the eastern Agassiz FZ (~40°S, 120°W) (Plate 1). Trough B is on the ANT plate south of the western Valdivia FZ A (~43°S, 101°W) (Plate 1). Evidence for troughs A and B are linear lows recorded in the satellite altimetry-derived gravity field (Plate 1). Troughs A and B will be shown to be adjacent in the chron 6(o) reconstruction, suggesting a conjugate relationship.

Methods

Using digitized magnetic anomaly and FZ data, we created reconstructions of the relative positions of the PAC, ANT, and NAZ (or FAR) plates for chrons 13, 10, 8, 6(o), 5C, 5(o), 3, and the Present (Table 1). These reconstruction ages were chosen because magnetics data were sufficient and because they illustrate the major southeast Pacific plate boundary reorganizations. To convey additional continuity of the tectonic evolution, schematic reconstructions for chrons 6C (24 Ma), 6AA (22 Ma), 5A (13 Ma), and 3B (7 Ma) were created by graphic interpolation, with reference to all available data.

Poles of Rotation

To create the reconstructions, PAC-ANT and NAZ (FAR)-ANT finite poles of rotation were needed for each reconstruction time to rotate the PAC and NAZ (FAR) plates back to their past positions relative to the (fixed) ANT plate. We will now discuss how the NAZ (FAR)-ANT and PAC-ANT poles were determined.

NAZ (FAR)-ANT finite poles (Chile ridge). Previous work on Neogene Chile ridge poles of rotation has been limited. The Chile ridge axis is shorter than most currently active major ridge systems, and the ridge has been located near the equators of the middle Miocene to recent poles

Table 1. Ages of Reconstructions

Chron	Position in Timescale*	Age, Ma*	Geologic Epoch
3	young edge of C3n.1n	4.03	early Pliocene
5(o)	old edge of C5n.2n	10.83	late Miocene
5C	young edge of C5Cn.1n	16.035	early Miocene/middle Miocene boundary
6(o)	old edge of C6n	20.162	early Miocene
8	young edge of C8n.1n	25.807	late Oligocene
10	young edge of C10n.1n	28.255	late Oligocene
13	young edge of C13n	33.05	early Oligocene

* *Cande and Kent* [1995].

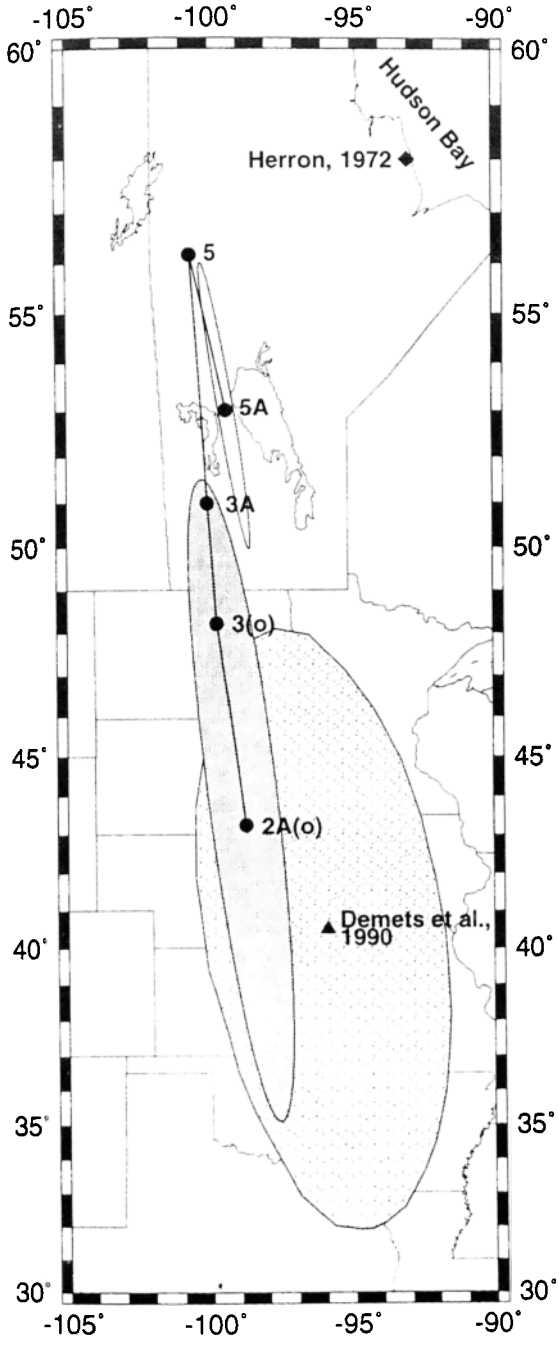

Figure 2. Chile ridge finite poles of rotation for chrons 2A, 3(o), 3A, 5, and 5A (solid circles). The 95% confidence regions (shaded) are shown for chrons 2A and 5A poles, which are distinct. Also shown is the recent pole of rotation (triangle) and 95% confidence interval of *DeMets et al.* [1990] and *Herron*'s [1972] Chile ridge pole of rotation (diamond).

of rotation; both factors limit the ability to constrain finite rotation poles. *Herron* [1972], noting a poor data distribution, determined a single NAZ-ANT finite pole at 58°N, 93°W for the evolution of the Chile ridge (Figure 2). "Present-day" NAZ-ANT relative motions have been determined, though poorly constrained, as part of global inversions for present-day plate motions [*DeMets et al.*, 1990, and references therein] (Figure 2). Other Neogene Chile ridge poles of rotation were determined by combining PAC-ANT and PAC-NAZ (East Pacific rise) poles of rotation [*Pardo-Casas and Molnar*, 1987], the latter of which are also poorly constrained due to a lack of data and the angular distance (90°) of the East Pacific rise from the PAC-NAZ pole of rotation.

Chron 13 to chron 6(o): FAR-ANT (Chile ridge) poles, for chrons 13, 10, 8, and 6(o), cannot be determined directly from data on the ANT and FAR plates, as almost all of the FAR plate formed at this ridge has been subducted. We first tried to obtain FAR-ANT finite poles of rotation for chrons 13, 10, and 6(o) by finite rotation addition and interpolation of ANT-PAC Euler poles [*Cande et al.*, 1995] to FAR-PAC Euler poles [*Pardo-Casas and Molnar*, 1987]. The interpolated chron 10 and chron 8 poles resulted in more than 80 km of mismatch along reconstructed FAR-PAC FZs and were not considered acceptable. New chron 10 and chron 8 FAR-PAC poles were determined by finding poles that, by visual inspection, provided the best reconstructed fit of the FZ and magnetic anomaly data. FAR-ANT poles for chrons 10 and 8 were then calculated by finite rotation addition of the new FAR-PAC pole to the corresponding PAC-ANT pole of *Cande et al.* [1995].

For chron 6(o) the FAR-PAC 6(m) pole of *Pardo-Casas and Molnar* [1987] was extrapolated to chron 6(o) and combined by finite rotation addition with the PAC-ANT chron 6(o) pole of *Cande et al.* [1995] to determine a NAZ-ANT chron 6(o) pole. The PAC-NAZ chron 6(m) pole of *Pardo-Casas and Molnar* [1987] is based on interpolation between their chron 7 pole (constrained by available data) and a chron 5 pole extrapolated from *Minster and Jordan*'s [1978] "present-day" pole, with a predicted mismatch of reconstructed features of as much as 200 km.

Chron 5A to Present: Finite poles of rotation for the Chile ridge since chron 5A were calculated using *Hellinger*'s [1981] method, which finds the rotation parameters (latitude, longitude, and angle) which minimize a weighted least squares measure of fit. Each pole was determined using magnetic anomaly and FZ picks from both sides of the ridge axis. Magnetic anomaly segments were defined by major FZs and by higher-order offsets [see *Macdonald et al.*, 1991]. FZ points located between the offset segments of the anomaly being determined were used. FZ points were digitized prior to availability of the Geosat geodetic mission (GM) data south of 30°S. Geosat GM data was used to revise the locations of the FZs presented in the tectonic maps and reconstructions, which resulted in a slight (< 5 km) deviation of some FZ picks from charted FZs.

The uncertainties in the pole of rotation were determined using the method developed by *Chang* [1987, 1988], *Chang et al.* [1990], and *Royer and Chang* [1991]. In this method a covariance matrix describes the uncertainties of a rotation. The uncertainties in each pole are independent of other poles. The relation of the assigned uncertainty estimate of each data point ($\hat{\sigma}$) to the true (scaled) estimate (σ) is $k = (\hat{\sigma} / \sigma)^2$, where the parameter k is unknown (in this notation, the circumflex stands for "estimate of" as opposed to "true value of"). The parameter $\hat{k}$, which indicates the correctness of the assigned uncertainties, is calculated from the misfit, the geometry of the plate boundary, and the number of data. The method of solution does not require that the estimated error uncertainties for the data be true estimates, only relatively correct (i.e., unscaled). Based on the above equation, the estimated uncertainties are underestimated if $\hat{k} < 1$, overestimated if $\hat{k} > 1$, or true if $\hat{k} = 1$ ($\hat{\sigma} = \sigma$). For the poles calculated in this paper,

Table 2. NAZ-ANT Finite Rotation Parameters

Chron	Age, Ma	Latitude +°N	Longitude +°E	Angle		df	*s*	*N*	*N*-FZ	*N*-Anom
				Degree	Degrees per Million Years					
				DeMets et al., 1990						
2A*	3	40.5	-95.9		0.54					
				This Paper						
2A(o)	3.553	43.13	-98.69	1.97	0.55	50	12	77	38	39
3(o)	4.930	48.23	-99.75	2.81	0.57	48	13	77	27	50
3A	6.378	50.98	-100.06	3.86	0.61	48	9	69	19	50
5	9.781	56.17	-100.66	6.54	0.67	20	6	35	8	27
5A	12.225	53.01	-99.39	8.31	0.72	13	4	24	14	10

Parameters are df, degrees of freedom; *s*, number of great circle segments; *N*, total number of data points (fracture zone plus magnetic anomaly); *N*-FZ, number of fracture zone data points, *N*-Anom, number of magnetic anomaly data points.

* Spreading rates of *DeMets et al.* [1990] used to constrain pole were determined using the center of anomaly 2A, corrsponding to 3.0 Ma. The inversion included four spreading rates, eight transform fault azimuths, and 51 earthquake slip vectors to constrain Nazca-Antarctic motion.

estimated uncertainties ($\hat{\sigma}$) were 2 km for anomaly picks and 5 km for FZ picks (Table 2). These estimates underestimated the uncertainties for the chron 5 pole ($\hat{k}$ = 0.84) and overestimated the uncertainties for the other four poles ($\hat{k}$ range from 1.6 to 2.39, Table 3).

NAZ-ANT finite poles of rotation and their 95% confidence regions are presented for chrons 2A (3.55 Ma), 3 (4.93 Ma), 3A (6.37 Ma), 5 (9.78 Ma), and 5A (12.22 Ma) (Tables 2 and 3 and Figure 2). From chron 5A to 2A the NAZ-ANT pole of rotation moved generally south, with the chron 5A and 2A poles distinct at the 95% confidence level (Figure 2). The relatively large error ellipse of the *DeMets et al.* [1990] recent (chron 2A to Present) NAZ-ANT pole includes our chron 2A pole (Figure 2). The accuracy of the Chile ridge poles is presented qualitatively in two ways. First, for each chron, anomaly picks were rotated about the pole from the ANT plate to their modeled conjugate position on the NAZ plate. Comparison of the location of the mapped anomaly points (Figure 3, open symbols) with the location of rotated points (Figure 3, solid symbols) demonstrates how well the poles fit the anomaly data. Second, as presented below, modeled flow lines were generated using stage poles and compared to mapped FZs.

PAC-ANT finite poles. The PAC-ANT poles of rotation of *Cande et al.* [1995] were used. These poles were also calculated using the method of *Chang and Royer* [*Chang*, 1987; *Chang et al.*, 1990; *Royer and Chang*, 1991] using data on the PAC and ANT plates (Table 4).

Modeled Flow Lines

The consistency of the determined poles with the charted FZ and anomaly data can be observed qualitatively in Figure 4, where modeled flow lines generated from stage poles are compared to charted FZs. Using the eight sets of finite rotation poles (Table 4), stage poles were calculated (Table 5).

The strike of model flow lines and predicted anomaly spacing compared to PAC-NAZ (FAR) and PAC-ANT FZs generally agree well (Figure 4). The modeled Chile ridge flow lines agree with the observed FZs from the Present (ridge axis) to chron 5C with respect to both strike and distance between magnetic anomalies (Figure 4). Older than chron 6(o), for Chile ridge spreading, only ANT plate seafloor is extant. FZs are only tentatively located (Plate 1 and Figure 4) and are based almost exclusively on satellite altimetry data [*Tebbens et al.*, this issue]. Modeled flow lines accurately predict the distance between the observed anomalies but not the strike of the charted FZs (Figure 4). For instance, along the Guamblin FZ there is an 18° discrepancy between the strike of the model flow line (N12°E) and the charted ANT-FAR FZs (N6°W), for the interval of chrons 10 to 13. The discrepancy between the observed and predicted strikes of the FZs may be due to inaccuracies in the FZ locations and/or errors in the chron 13 through chron 8 ANT-FAR poles of rotation. *Weissel et al.* [1977] examined two magnetics profiles from the Chile ridge south of 50°S. For the interval of chrons 13 to 8, on the ANT plate, they predicted a spreading rate (3.8 cm/yr) 2 times faster than observed (1.9 cm/yr). They suggested the discrepancy could be due to highly asymmetrical spreading (50% asymmetrical spreading), or the existence of an additional plate in the region ("a fourth plate and two triple junctions" [*Weissel et al.*, 1977, p. 254]). Based on the *Cande and Kent* [1992] timescale, for the interval of chrons 13 to 8 we adjusted the observed spreading rate of *Weissel et al.* [1977] from 1.9 to 2.4 cm/yr. For this region (~58°S, ~78°W), using a single-

Table 3. NAZ-ANT Finite Rotation Poles and Their Covariance Matrices

Chron	Latitude +°N	Longitude +°E	Angle deg	$\hat{k}$	*a*	*b*	*c*	*d*	*e*	*f*	*g*
2A(o)	43.26	-98.75	1.97	1.90	0.182	0.142	1.24	0.159	1.22	1.20	10^{-3}
3(o)	48.23	-99.75	2.81	2.00	0.216	0.102	1.12	0.128	1.10	1.08	10^{-3}
3A	50.98	-100.06	3.86	1.60	0.341	0.449	1.50	0.456	1.48	1.46	10^{-3}
5	56.17	-100.66	6.54	0.84	0.787	0.923	3.16	0.911	3.03	2.91	10^{-3}
5A	53.01	-99.39	8.31	2.39	0.148	0.346	1.78	0.319	1.71	1.71	10^{-3}

Variables $\hat{k}$, *a*, *b*, *c*, *d*, *e*, and *f* are in radians. The covariance matrix is defined as $\mathrm{Cov}(\mathbf{u}) = \frac{(1)}{(\hat{k})}\begin{pmatrix} a & b & d \\ b & c & e \\ d & e & f \end{pmatrix} g$.

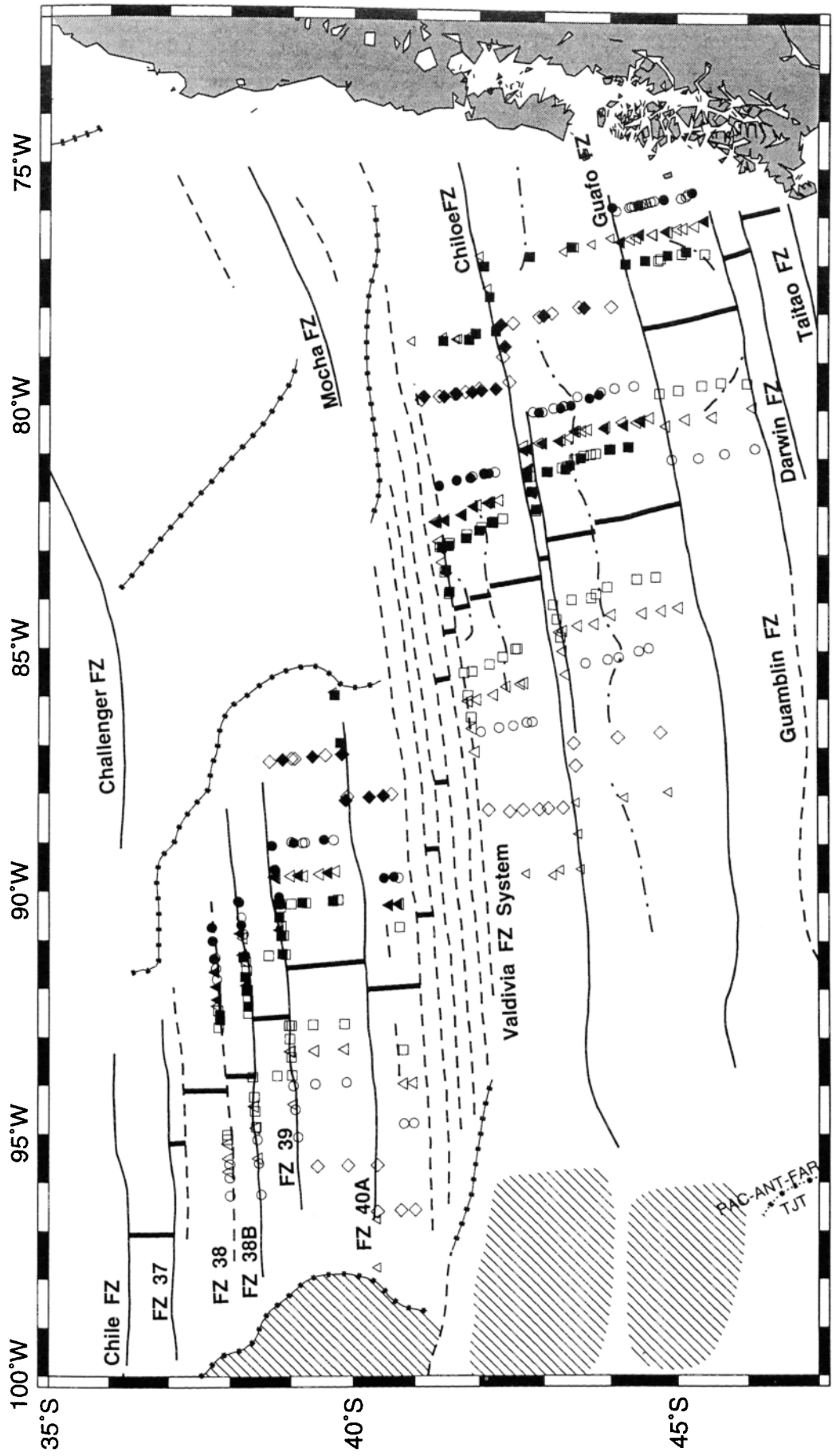

Figure 3. Magnetic anomaly (open symbols) and FZ data (solid lines) are shown. ANT plate anomaly points rotated to the NAZ plate (solid symbols) agree with the nonrotated NAZ plate anomaly points. Tectonic features are as in Plate 1.

Table 4. Finite Poles of Rotation

Chron	Time, Ma	Latitude +°N	Longitude +°E	Angle	Reference
			Farallon/Nazca–Antarctic		
2A(o)	3.55	43.13	-98.69	-1.97	*Tebbens* [1994] and this work
3*	4.03	45.32	-99.13	-2.26	interpolate 3(o) & 2A(o)
3(o)	4.93	48.23	-99.75	-2.81	*Tebbens* [1994] and this work
5(o)*	10.83	52.66	-99.42	-7.26	interpolate 3(o) and 5A
5A	12.22	53.01	-99.39	-8.31	*Tebbens* [1994] and this work
5C*	16.04	53.01	-99.39	-11.10	adjusted† 5A
6(o)*	20.16	46.64	-97.33	-15.22	sum Naz-Pac and Pac-Ant
8*	25.81	51.10	-98.30	-20.70	sum Far-Pac and Pac-Ant
10*	28.26	55.21	-104.50	-22.15	sum Far-Pac and Pac-Ant
13*	33.05	55.43	-117.59	-23.68	sum Far-Pac and Pac-Ant
			Pacific–Antarctic		
3*	4.03	66.65	-78.59	3.69	adjusted† 3.1
3.1	4.08	66.65	-78.59	3.74	*Cande et al.* [1995]
5(o)*	10.83	70.61	-76.87	9.58	*Cande et al.* [1995]
5B	15.10	72.47	-74.22	12.93	*Cande et al.* [1995]
5C*	16.04	72.95	-72.76	13.76	interpolate 5B and 5D
5D	17.48	73.56	-70.72	15.04	*Cande et al.* [1995]
6(o)*	20.16	74.02	-69.51	16.88	*Cande et al.* [1995]
8*	25.81	74.66	-69.38	20.81	*Cande et al.* [1995]
9(o)	27.95	74.38	-69.79	22.11	*Cande et al.* [1995]
10*	28.26	74.37	-69.52	22.44	interpolate 9(o) and 13
13*	33.05	74.44	-64.12	27.07	*Cande et al.* [1995]
			Pacific–Farallon/Nazca		
6(o)	20.16	62.38	-93.02	31.01	adjusted† *Pardo-Casas and Molnar* [1987] 6(m) pole
6(m)	19.62	62.38	-93.02	30.18	*Pardo-Casas and Molnar* [1987]
7	24.83	63.88	-94.75	38.81	adjusted† 7(m)
7(m)	25.00	63.88	-94.75	39.08	*Pardo-Casas and Molnar* [1987]
8	25.81	64.49	-94.60	40.39	this work
10	28.26	66.91	-98.30	43.64	this work
10(m)	28.49	67.34	-100.08	43.77	*Pardo-Casas and Molnar* [1987]
13	33.05	69.74	-105.82	49.24	interpolate 13(m) and 10(m)
13(m)	33.30	69.85	-106.13	49.54	*Pardo-Casas and Molnar* [1987]

* Poles used for the plate reconstructions.
† "Adjusted" poles have the same geographic coordinates; the rotation angle is scaled by the age ratio.

stage pole calculated from our chron 13 and chron 8 ANT-FAR finite poles, we predict an average spreading rate for this interval of 2.6 cm/yr, which is only 8% more than our observed rate (2.4 cm/yr). This discrepancy could be explained by 4% asymmetrical spreading, faster on the FAR plate, which is well within the observed rates of asymmetrical spreading observed on the Mid-Atlantic Ridge [*Carbotte et al.*, 1991] and Chile ridge [*Tebbens*, 1994]. The reduction of the discrepancy between observed and predicted ANT-FAR spreading rates suggests it is unnecessary to call upon unusual tectonic conditions, such as highly asymmetric spreading or a fourth plate, to explain the tectonic evolution of this region.

In summary, the relative motions of the southeast Pacific plates appear to be well modeled by the rotation vectors. The only exception is a mismatch (up to 20°) in the strike of the observed and modeled ANT-FAR FZs in crust formed between chrons 6(o) and 13. Care should therefore be taken not to overinterpret the strike of the Chile ridge and its FZs, for this time interval, in the tectonic reconstructions (Figure 5).

Triple Junctions and Velocity Triangles

Velocity triangles were constructed for various possible triple junction geometries for several intervals (Figure 5, insets) [after *McKenzie and Morgan*, 1969]. Unless otherwise noted, we assume that: (1) ridge axes spread symmetrically; (2) ridge axes are perpendicular to spreading direction; (3) transform faults are purely strike-slip boundaries; and (4) plates are rigid. A velocity triangle represents instantaneous relative plate motion during a short interval of geologic time (stage) [*McKenzie and Morgan*, 1969; *Patriat and Courtillot*, 1984]. Ridge-ridge-ridge (RRR), ridge-ridge-transform fault (RRF), RFF, and FFF are all the possible mid-ocean triple junction geometries (excluding subduction zones). When the above stated assumptions are true, a RRR triple junction is always stable and a RRF triple junction is always unstable [*McKenzie and Morgan*, 1969]. In the velocity triangles the lines pac-ant, pac-far (or pac-naz), and ant-far (or ant-naz) represent velocities which do not change the geometry of the boundary between the PAC and ANT plates, the PAC and FAR (or NAZ) plates, and the ANT and FAR (or NAZ) plates, respectively. In a velocity triangle, only when the lines, pac-ant, pac-far (or pac-naz), and ant-far (or ant-naz) intersect at a single point can the velocity of the triple junction be determined and the triple junction be considered stable. We consider an RRF triple junction "nearly stable" if either 15% or less asymmetrical spreading at the ridge axis or a 4° or less change in the strike of one of the transform boundaries would

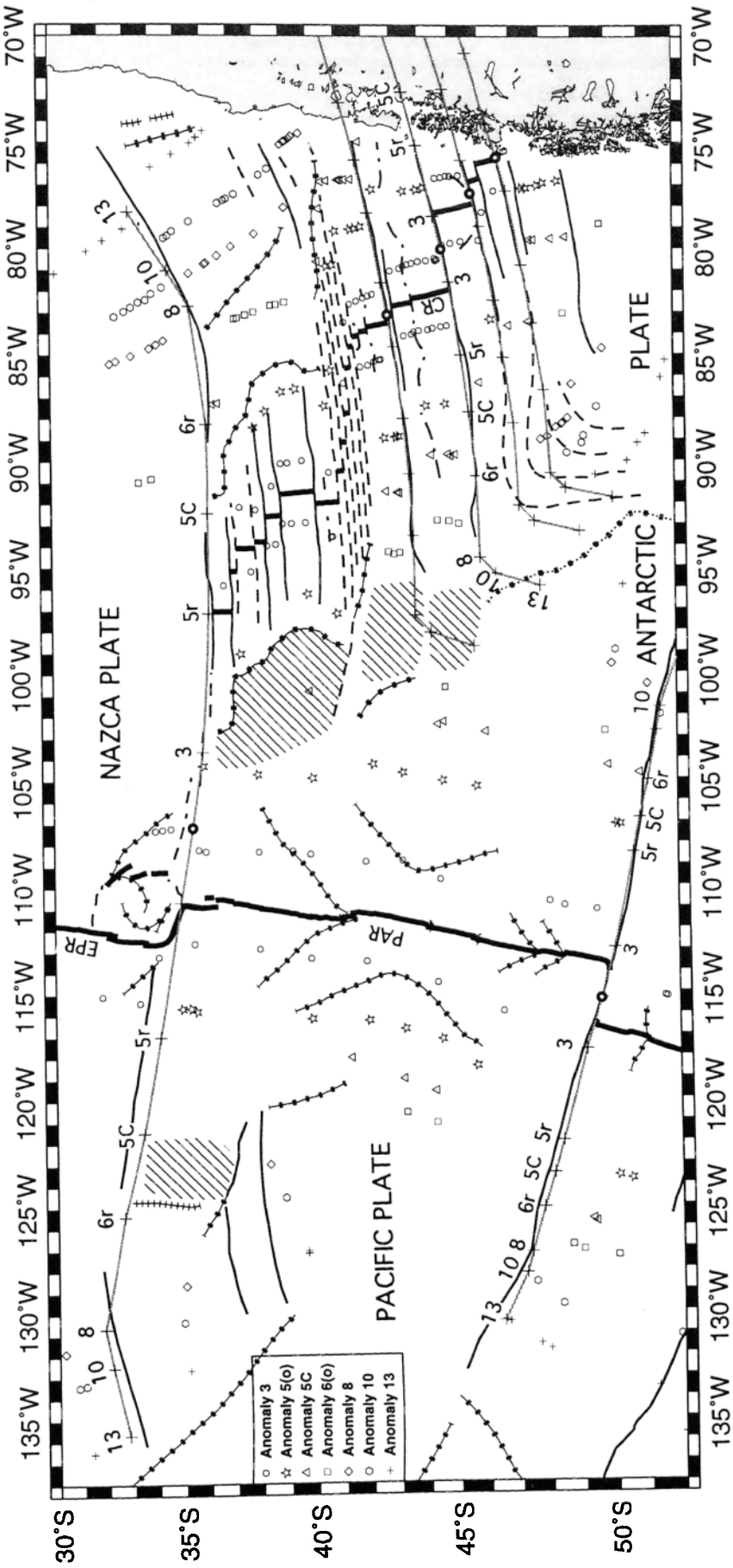

Figure 4. Location of observed FZs (solid and dashed lines) are compared with modeled flow lines (shaded lines) based on the stage poles in Table 5. Flow lines originate at open circles; large crosses mark the endpoints for each interval (stage); symmetrical spreading is assumed. If the stage poles are correct, the strike of the modeled flow lines and observed FZs should correspond. Tectonic features are as in Plate 1.

Table 5. South Pacific Stage Poles Used for the Reconstructions

	NAZ-ANT Plate Boundary					
	Nazca Fixed			Antarctic Fixed		
Chron Interval	Latitude (+°N)	Longitude (+°E)	Angle	Latitude (+°N)	Longitude (+°E)	Angle
3 - Present	45.32	-99.13	-2.26	45.32	-99.13	2.26
5(o) - 3	55.94	-99.21	-5.03	55.93	-99.96	5.03
5C - 5(o)	53.68	-99.22	-3.84	53.69	-99.44	3.84
6(o) - 5C	29.98	-96.21	-4.38	30.64	-91.22	4.38
8 - 6(o)	63.27	-97.44	-5.65	62.39	-106.76	5.65
10 - 8.	61.57	141.97	-2.52	49.27	164.18	2.52
13 - 10	29.52	165.17	-3.33	17.07	-177.36	3.33
	ANT-PAC Plate Boundary					
	Antarctic Fixed			Pacific Fixed		
Chron Interval	Latitude (+°N)	Longitude (+°E)	Angle	Latitude (+°N)	Longitude (+°E)	Angle
3 - Present	66.65	-78.59	-3.69	66.65	-78.59	3.69
5(o) - 3	72.60	-75.05	-7.15	72.68	-76.34	7.15
5C - 5(o)	78.92	-40.30	-2.99	80.89	-47.11	2.99
6(o) - 5C	77.04	-47.62	-3.14	78.64	-51.69	3.14
8 - 6(o)	77.01	-60.39	-3.94	77.58	-64.65	3.94
10 - 8.	70.99	-83.29	-1.64	69.80	-78.28	1.64
13 - 10	71.58	-42.25	-4.67	74.57	-37.88	4.67
	PAC-NAZ Plate Boundary					
	Nazca Fixed			Pacific Fixed		
Chron Interval	Latitude (+°N)	Longitude (+°E)	Angle	Latitude (+°N)	Longitude (+°E)	Angle
3 - Present	59.13	-89.78	-5.83	59.13	-89.78	5.83
5(o) - 3	66.17	-91.69	-10.77	66.03	-93.43	10.77
5C - 5(o)	68.44	-91.45	-7.82	68.21	-95.11	7.82
6(o) - 5C	52.82	-100.00	-6.77	52.18	-91.10	6.77
8 - 6(o)	71.69	-94.25	-9.48	69.56	-107.81	9.48
10 - 8.	80.49	122.13	-3.84	64.54	-178.93	3.84
13 - 10	78.34	138.46	-6.40	61.75	-173.61	6.40

NAZ-ANT and ANT-PAC stage poles were calculated using finite poles shown in Table 4. PAC-NAZ finite poles were determined by finite rotation addition of the NAZ-ANT and ANT-PAC finite poles shown in Table 4. These finite poles were used to calculate the stage poles for this table.

result in a stable triple junction. A primary use of the velocity triangles was to determine whether any triple junction geometry was "stable" and consistent with the available data. A "stable" triple junction is probably still migrating (at a constant, relatively slow velocity), and the plate boundaries are not undergoing major reorganizations (as they are during a stepwise triple junction migration.)

Reconstructions

We first present the reconstruction figures, with data, to clearly document the constraints of the data on the reconstructions (Figure 5). We then review the major southeast Pacific tectonic events since late Oligocene, with primary reference to a summary figure (Figure 6).

Chron 13 to Chron 10

The positions of the PAC, ANT, and FAR plates in early Oligocene (chron 13, 33.05 Ma) and late Oligocene (chron 10, 28 Ma) are presented (Figures 5a and 5b). The PAC-ANT, PAC-FAR, and ANT-FAR ridges are well-constrained by magnetic anomaly picks for the ridge segments a few hundred kilometers from the PAC-ANT-FAR triple junction. Near the triple junction, the data are scarce and the triple junction location is constrained to broad regions of roughly 170,000 km^2 at chron 13 and 270,000 km^2 at chron 10. We have presented the triple junction geometries at chrons 13 and 10 as RRR, which is stable for the interval of chron 13 to chron 10, but note that the available tectonic data do not preclude an RFF geometry, which is found to be "nearly stable" (Figure 5b, inset).

At chron 10 the Resolution FZ on the PAC plate and the Challenger FZ on the FAR plate reconstruct to one continuous short-offset FZ of the PAC-FAR ridge, as was previously shown by numerous authors including *Handschumacher* [1976], *Weissel et al.* [1977] and *Goodwillie and Parsons* [1992] (Figure 5b).

The Del Cano lineament, located south of the Resolution FZ

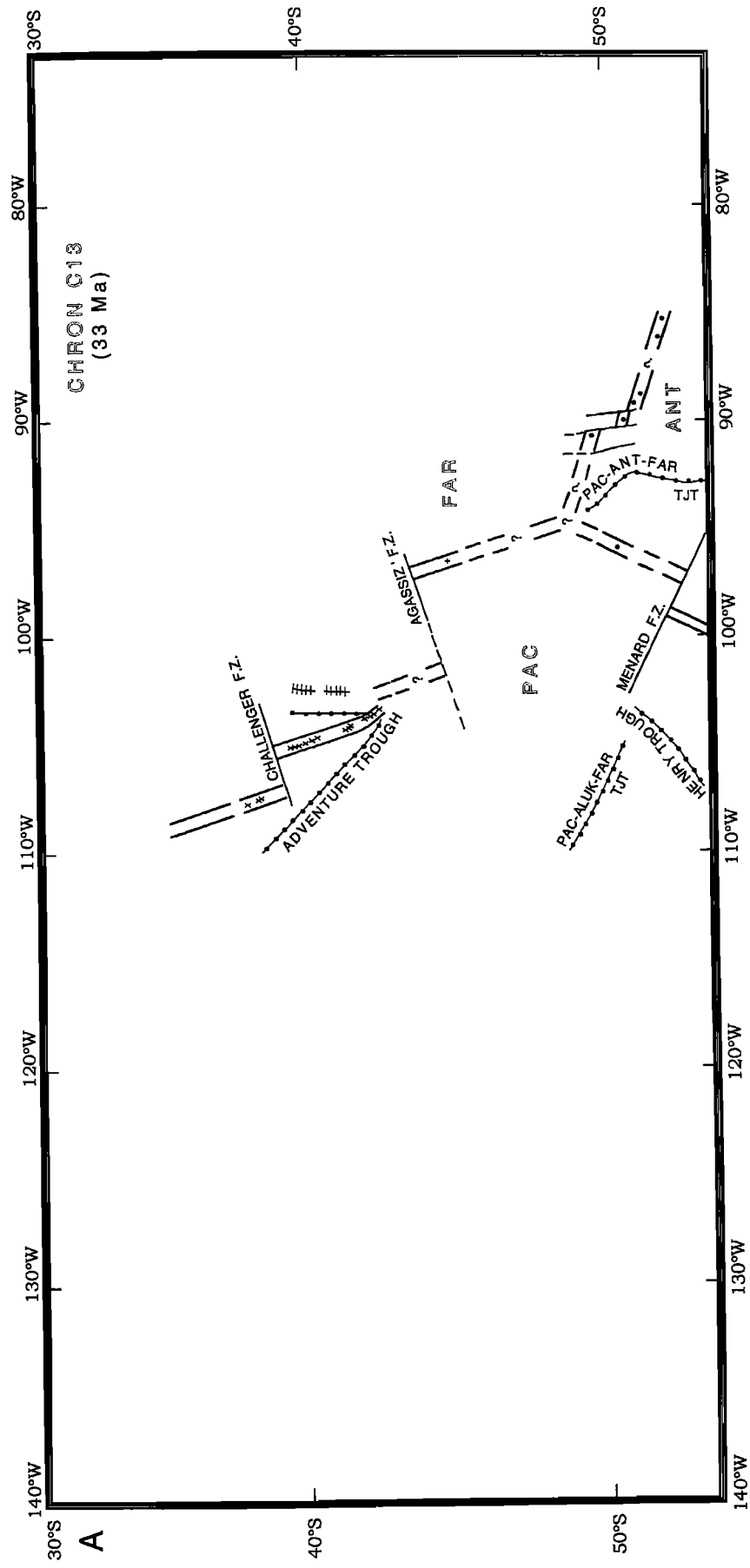

Figure 5. Reconstruction at (a) chron 13 (33 Ma); (b) chron 10 (28 Ma); (c) chron 8 (26 Ma); (d) chron 6(o) (20 Ma); (e) chron 5C (16 Ma); (f) chron C5(o) (11 Ma); (g) chron 3 (4 Ma); and (h) Present. Pairs of parallel lines denote ridge axes. Solid and dashed lines denote observed and extrapolated FZs, respectively. Lines with dots denote tectonic discontinuities, as labeled. "TJT" denotes triple junction trace. Line with hachures (RR track) denotes failed ridge. Hachured regions are transferred lithosphere (microplate cores). Sources for interpretation as in Plate 1. The ANT plate is fixed. Dots, pluses, and crosses denote magnetic anomaly picks from the ANT, PAC, and NAZ plates, respectively. Insets show stable and "nearly stable" ridge geometries and their associated velocity triangles for the intervals indicated. Each velocity triangle is created for a location near the triple junction. The a.s. denotes the magnitude of asymmetrical spreading along the ridge axis necessary to make the triple junction stable. ¥ denotes the magnitude of change in strike necessary to make two transform faults parallel.

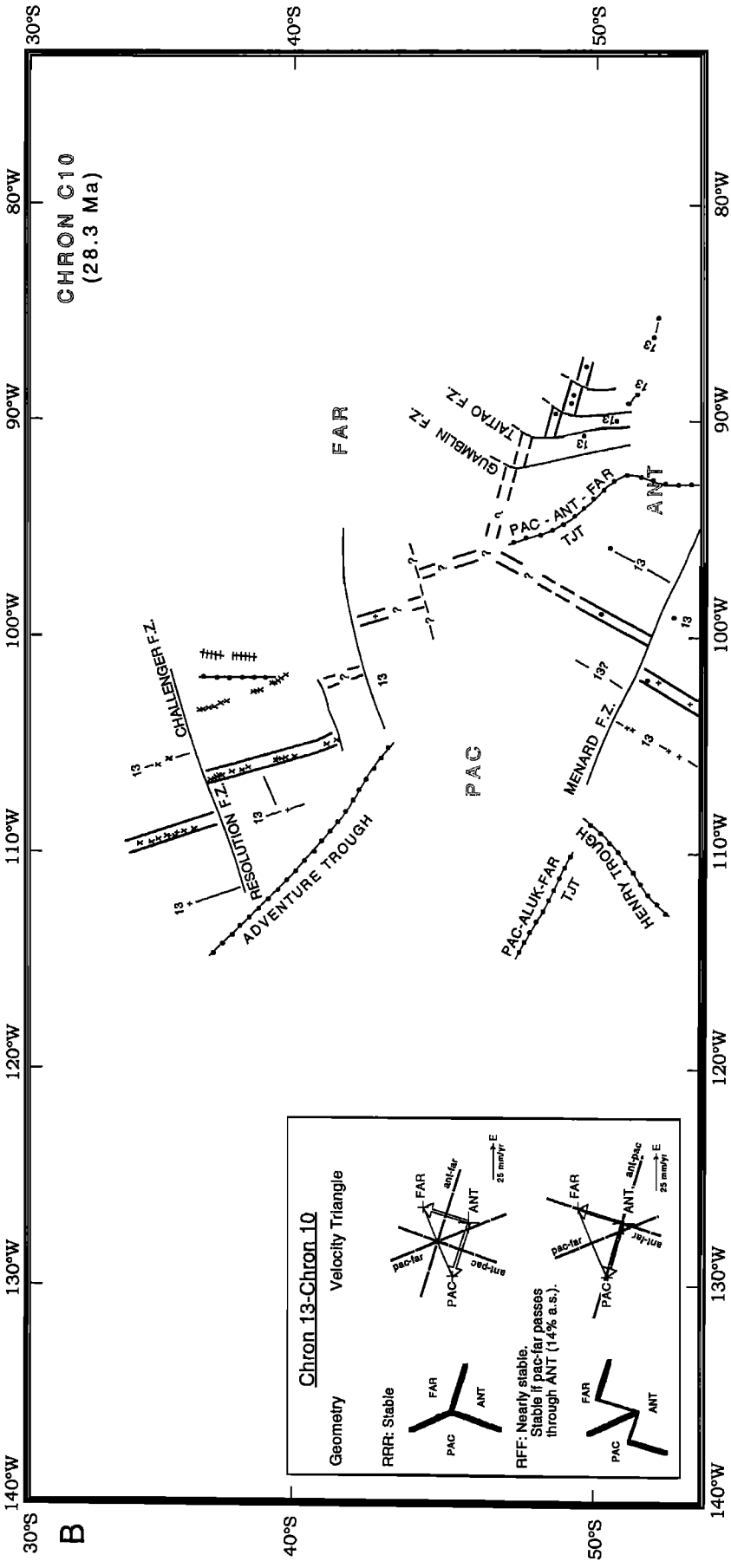

Figure 5. (continued)

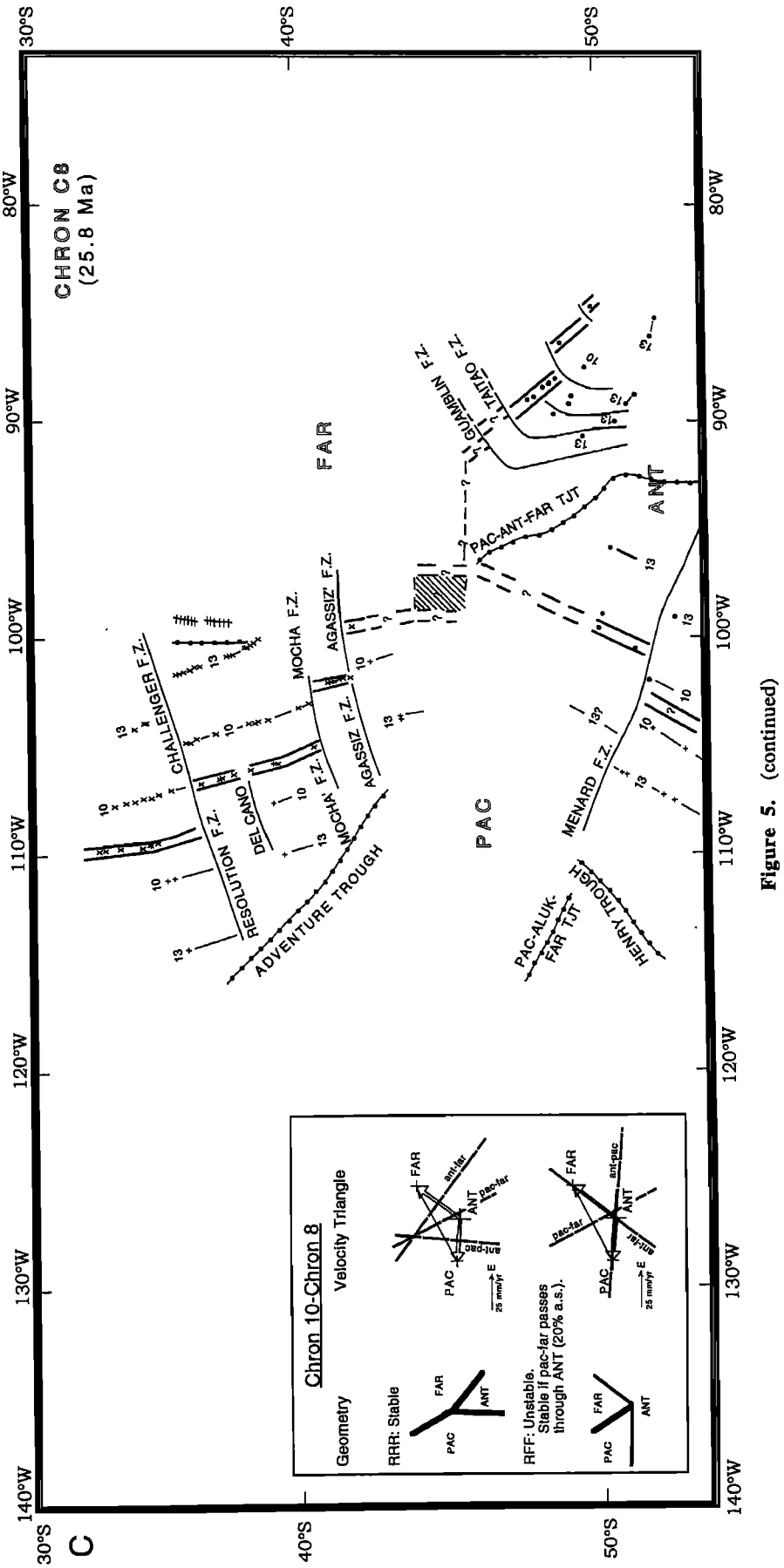

Figure 5. (continued)

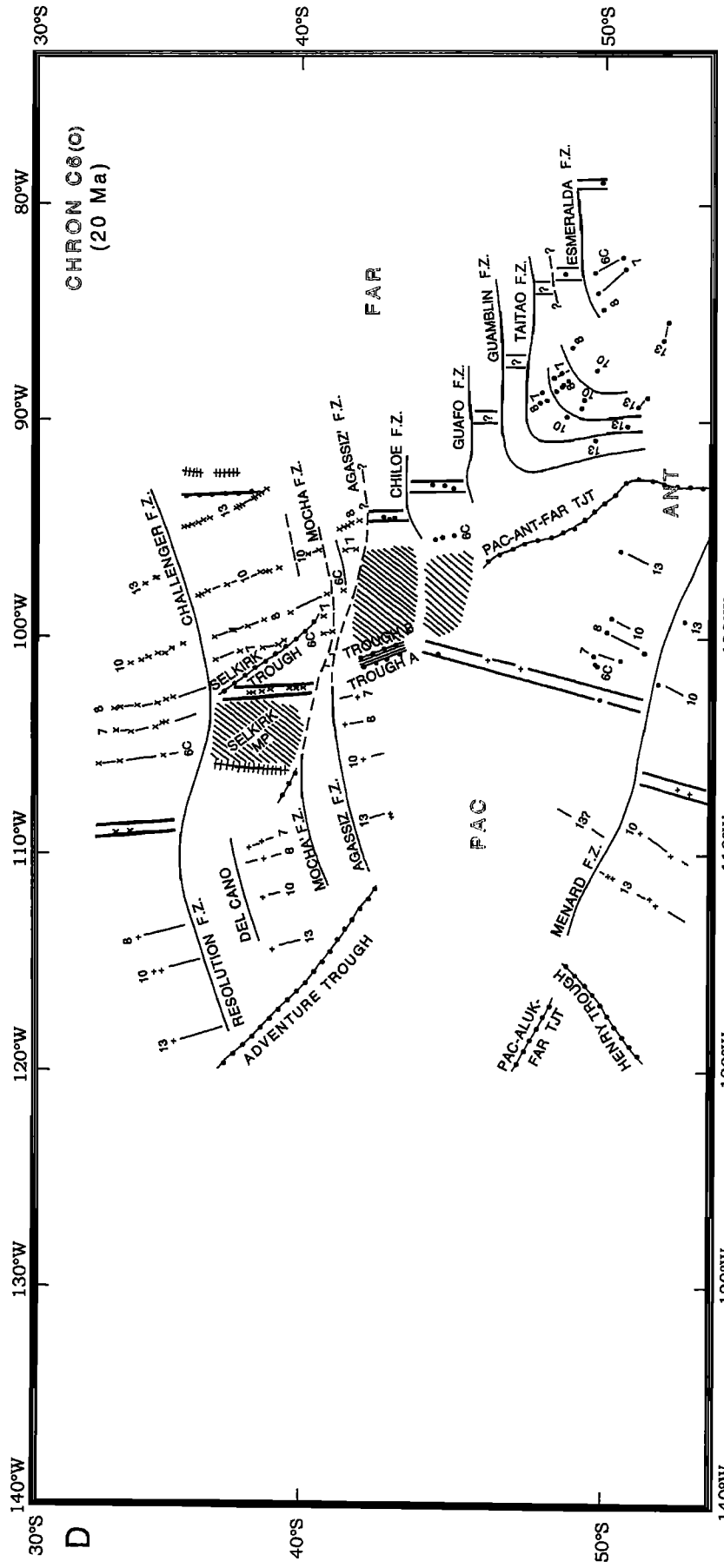

Figure 5. (continued)

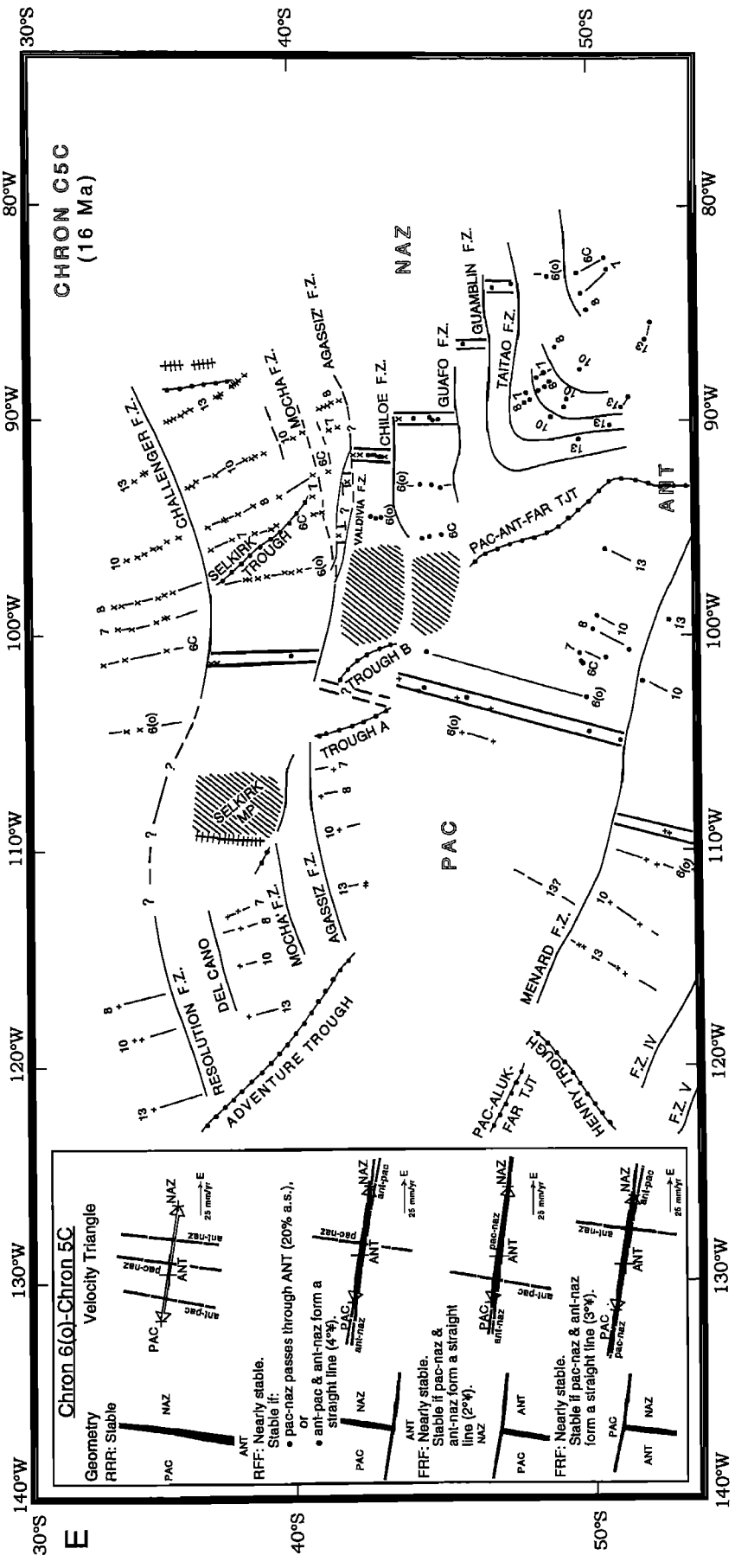

Figure 5. (continued)

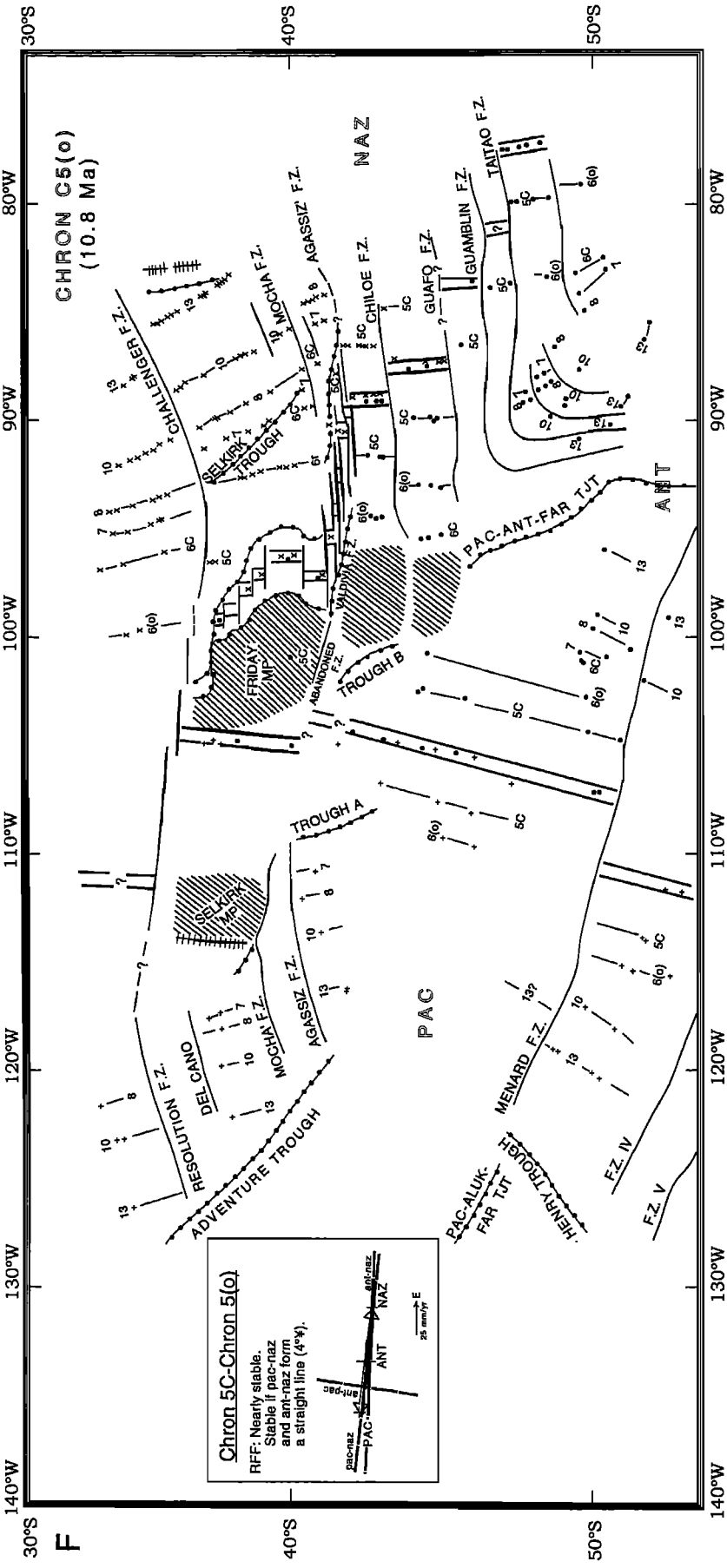

Figure 5. (continued)

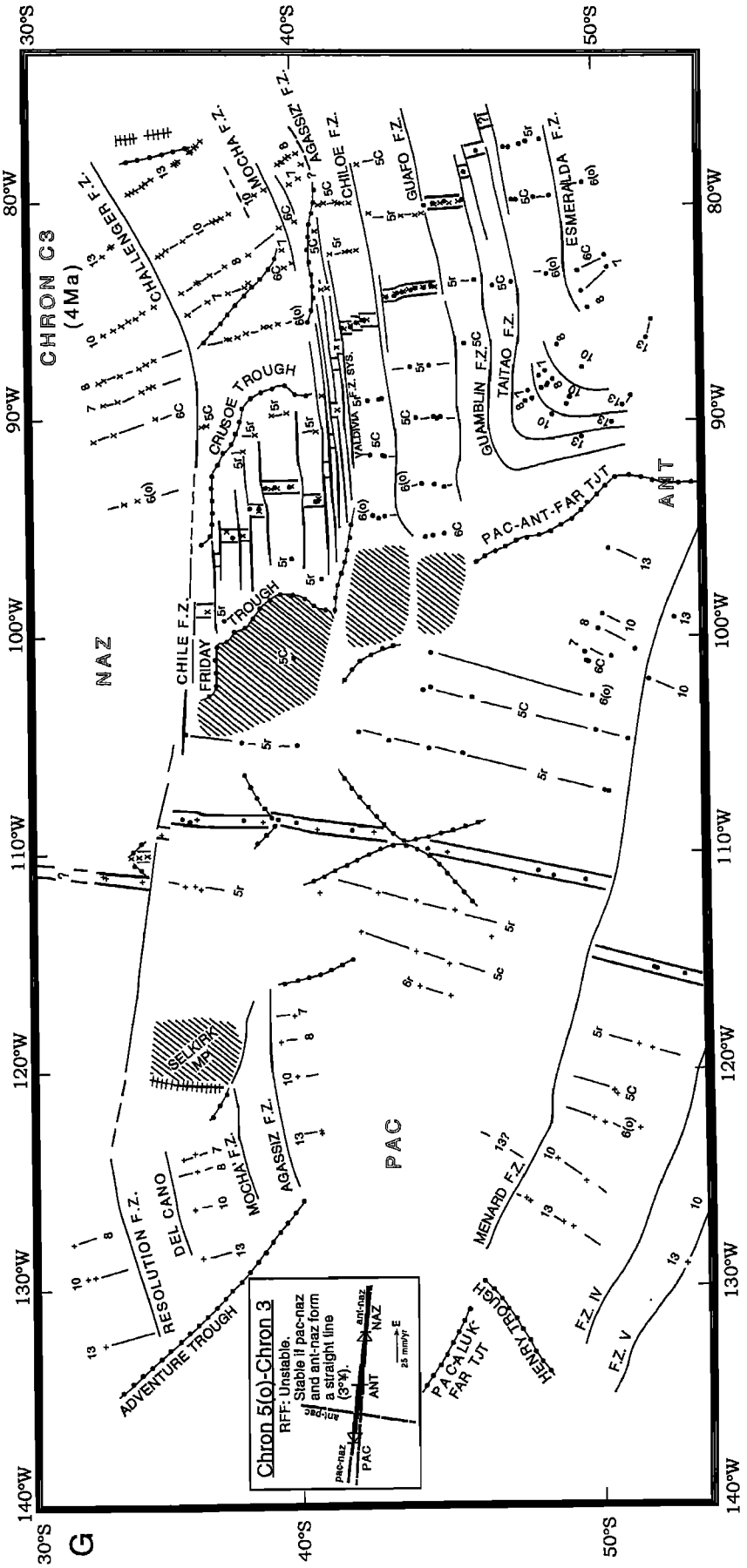

Figure 5. (continued)

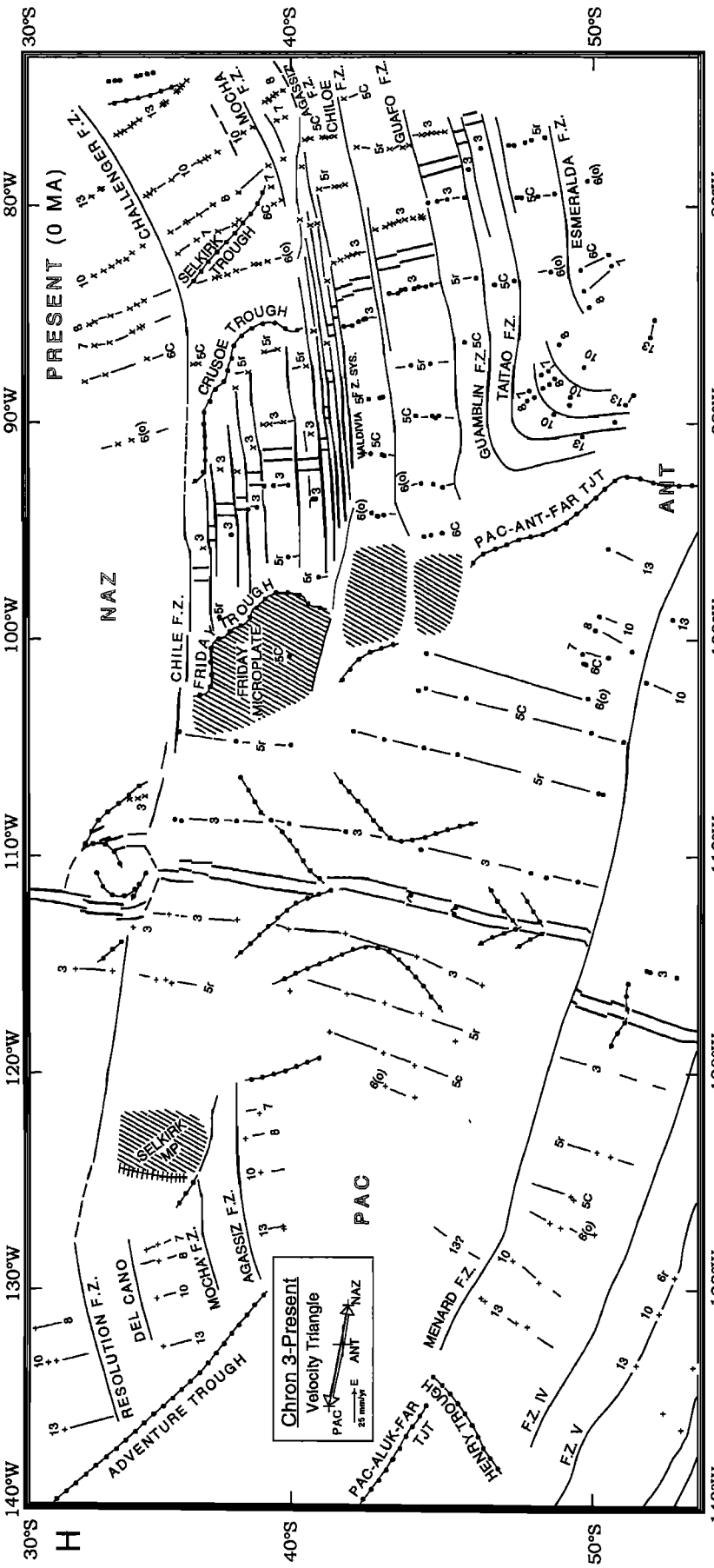

Figure 5. (continued)

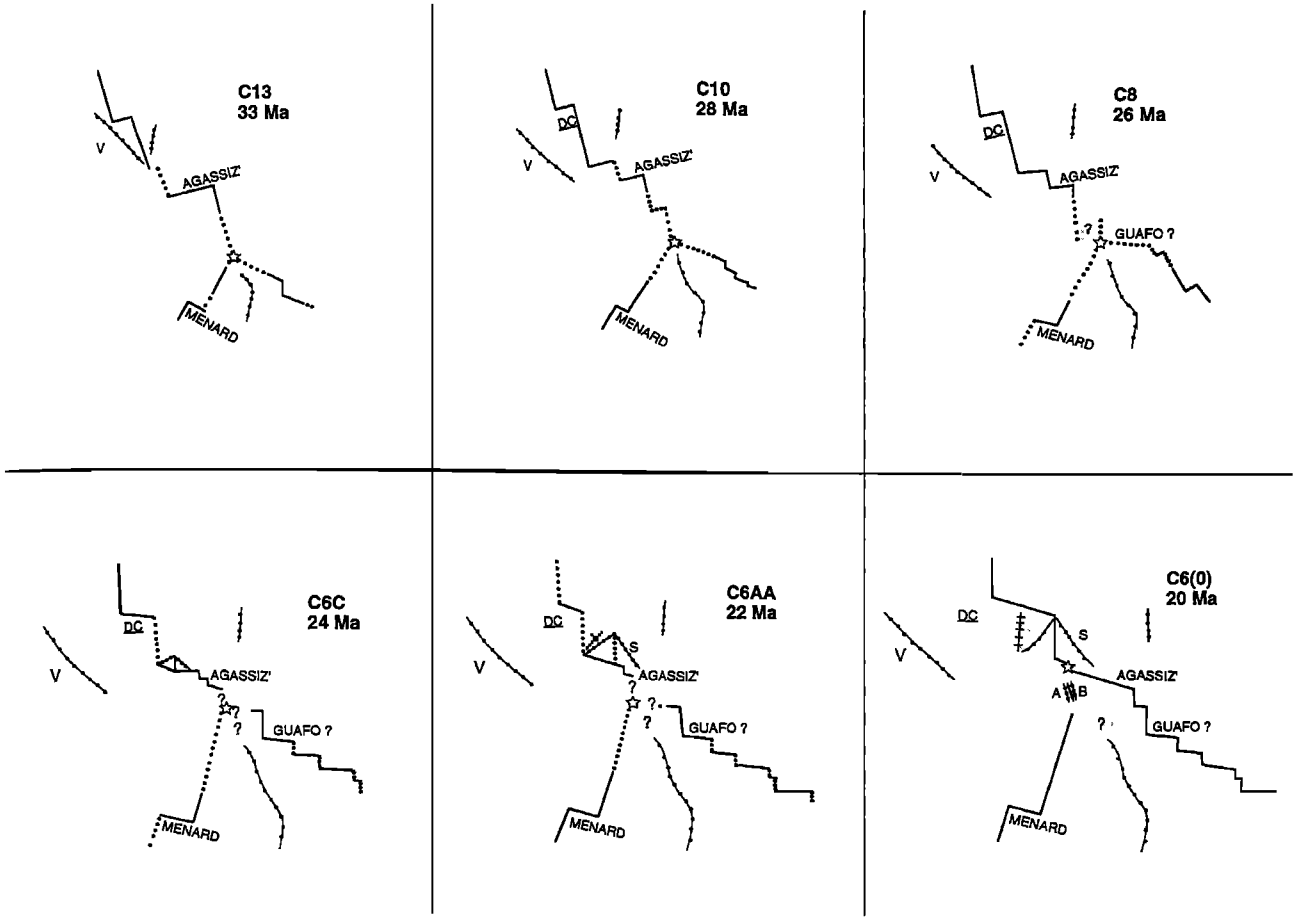

Figure 6. Schematic representation of evolution of the southeast Pacific from chron 13 to Present based on tectonic reconstructions of Figure 5 with chrons 6C, 6AA, 5A, and 3B determined by graphic interpolation. "S" is Selkirk trough, "A" is trough A, "B" is trough B, "V" is the Adventure trough, "DC" is Del Cano lineament, "VFZ" is Valdivia FZ system, "C" is Crusoe trough, "F" is Friday trough, and "JF" is Juan Fernandez microplate. Shaded regions are transferred lithosphere. Dotted lines and question marks denote speculative interpretation. See text for discussion.

on the PAC plate, is present in roughly chron 11 to chron 7 crust of the PAC plate (Plate 1 and Figure 4). *Mammerickx* [1992] suggested this feature is a FZ; however, there is no conjugate feature apparent on the FAR plate and an alternate interpretation is needed.

Chron 10 to Chron 8

The triple junction geometry at chron 8 is poorly constrained in the reconstructions. The magnetics and FZ data in the chron 8 reconstruction, while not definitive, suggest that the Chile ridge was separated from the PAC-ANT and PAC-FAR ridge axes by a large-offset transform (Figure 5c). Velocity triangles for the interval of chrons 10 to 8 indicate that only an RRR triple junction would be stable (Figure 5c, inset). Thus the data suggest the triple junction was unstable between chrons 10 and 8. An RFF triple junction would have been stable with 20% asymmetrical spreading on the PAC-FAR ridge (Figure 5c, inset). An RFF triple junction geometry would have been similar to the present-day PAC-ANT-NAZ triple junction in that a long transform fault (then the Guafo FZ, currently the Chile FZ) would have connected the Chile ridge to the triple junction. It is possible that in the region north of this triple junction, where the magnetics are indecipherable [*Tebbens et al.*, this issue], an additional paleoplate is preserved with an evolution analogous to that proposed above for the present-day Juan Fernandez microplate. This speculative paleoplate is tentatively presented in the reconstructions (Figures 5c and 6).

Chron 8 to Chron 6(o)

The Resolution and Challenger FZs to the north and the Agassiz and Mocha FZs to the south have previously been interpreted as conjugate pairs [*Handschumacher*, 1976; *Goodwillie and Parsons*, 1992]. *Handschumacher* [1976] observed that distances between conjugate FZs on the PAC and FAR plates were not always equivalent. One such discrepancy was in the distance between the Resolution and Agassiz FZs of the PAC plate and the Challenger and Mocha FZs of the FAR plate [*Handschumacher*, 1976]. Additional data support an alternative interpretation: the distance between the Resolution and Agassiz FZs is 720 km, while the distance between the Challenger and Mocha FZs is only 580 km (Plate 1). Additional FZs, the newly charted Agassiz' and Mocha' FZs, apparent in the satellite altimetry-derived gravity field, provide a simple solution. The distance between the Resolution FZ and Mocha' FZ is 570 km, a reasonable match

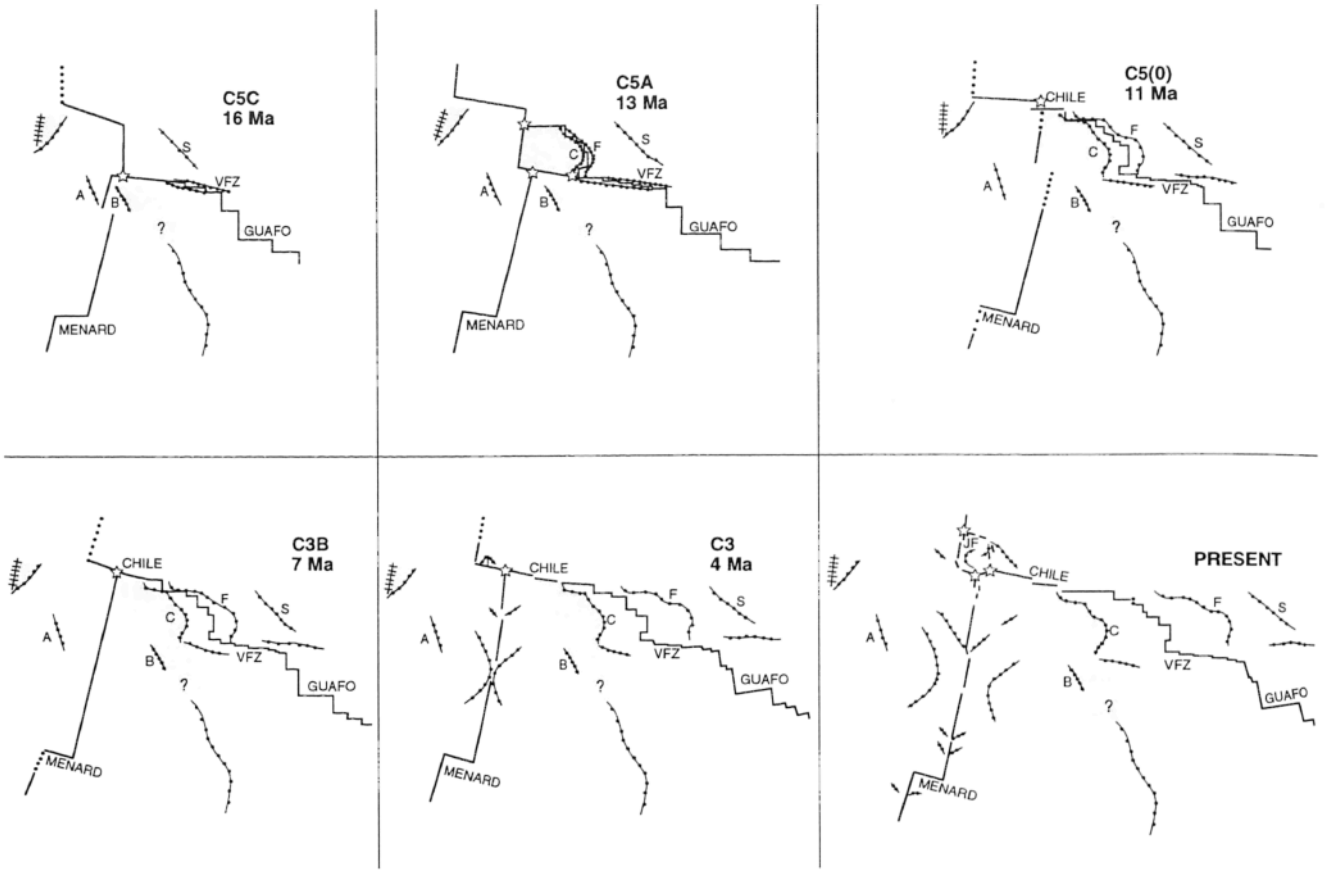

Figure 6. (continued)

to the 580 km between the Challenger and Mocha FZs. The distance between Mocha' and Agassiz and between the Mocha and Agassiz' are both 190 km. Thus the conjugate to the Mocha FZ on the FAR plate is the newly charted Mocha' FZ on the PAC plate and the conjugate to the Agassiz FZ on the PAC plate is the newly charted Agassiz' FZ on the NAZ plate (Figures 5c and 5d).

Chron 5C

The reconstructed anomaly and FZ data suggest that the triple junction at chron 5C is either RRF or RFF (Figure 5e). RFF geometry is presented, as this is the only geometry consistent with the data and associated with a nearly stable velocity triangle (Figure 5e, inset). The PAC-NAZ ridge orientation is poorly constrained, based on three anomaly picks located south of the Challenger FZ. The PAC-NAZ ridge orientation differs from the strike predicted by both the chron 6(o) to 5C and the chron 5C to 5(o) velocity triangles. The initiation of spreading within the Valdivia FZ system (the separated Agassiz-Agassiz' FZ) at chron 5C is discussed by *Tebbens et al.* [this issue].

Chron 5(o)

There are no data in the study region to constrain the location of the PAC-NAZ ridge axis at chron 5(o) (Figure 5f). The location of chron 5(o) observed farther north [*Cande et al.*, 1989] has been extrapolated southward, assuming a linear ridge with no offsets and using the strike predicted by the chron 5(o) to chron 3 velocity triangle (Figure 5f, inset). If this location is correct, at chron 5(o) the southernmost segment of the PAC-NAZ ridge was west of the northernmost PAC-ANT ridge and the PAC-ANT-NAZ triple junction had an RFF geometry. An RFF geometry was nearly stable for the interval of chrons 5C to 5(o).

Chron 5(o) to Present

Along the PAC-ANT ridge, several propagating ridge axes have evolved since chron 5(o) and have formed pseudofaults [*Lonsdale*, 1994] (Figures 5f-5h). The pseudofaults are evident in the satellite altimetry-derived gravity field (Plate 1). Some of these propagators may still be active today [*Lonsdale*, 1994]. Near the PAC-ANT-NAZ triple junction, shortly before chron 3, the Juan Fernandez microplate was born (modified from *Larson et al.* [1992]) (Figures 5g and 5h). The plate geometries near the triple junction are well-constrained for these reconstructions and the PAC-ANT-NAZ velocity triangles are presented (Figures 5f-5h, insets)

Discussion

Tectonic Evolution

The reconstructions presented above, augmented with four reconstructions made by graphic interpolation, are used to prepare a summary figure of the tectonic evolution of the southeast Pacific from late Oligocene to Present (Figure 6) which we will examine with a focus on changes in plate boundaries.

Pre-chron 13. Prior to late Eocene, the Henry trough on the west (PAC) flank of the PAC-ANT ridge (Plate 1), and its conjugate, the Hudson trough on the ANT plate (southeast of

Plate 1 and Figures 5 and 6), formed. Both are observed as lows in the satellite altimetry-derived gravity field (Hudson trough can be observed in the world gravity field [*Sandwell,* 1993]). To the west of the Henry trough are chron 28 and progressively older anomalies; to the east of the Hudson trough are chron 27 and a sequence of younger anomalies [*Cande et al.,* 1982, 1989]. These observations were part of the evidence that led *Cande et al.* [1982] to conclude that at chron 21 (47 Ma) the PAC-ANT ridge propagated northward through PAC plate crust formed at the PAC-Aluk spreading center roughly 10 Myr earlier. The Henry and Hudson troughs are the pseudofaults of this propagation event. The chron 21 reorganization is mentioned because, as will be shown, the chron 5A and perhaps 6(o) plate boundary reorganizations were similar in that (1) a ridge axis propagated and transferred crust from one plate to another; and (2) both the propagating ridge (new PAC-ANT ridge) and overlapped ridge (PAC-Aluk prior to propagation; ANT-Aluk after propagation) continued spreading. However, the chron 21 reorganization was unique in that it changed the geometry of a four-plate system with the extinction of two triple junctions and formation of two new triple junctions [*Cande et al.,* 1982].

Chron 13. At chron 13 a ridge propagated along the southernmost PAC-FAR ridge. Across the Adventure trough, a pseudofault of this propagation event, there is a gap in the magnetic anomaly sequence, for instance from chron 13 to chron 20, with 250-350 km of crust missing [*Cande and Haxby,* 1991]. In the conjugate position on the Nazca plate, *Cande and Haxby* [1991] found evidence for a 50-km ridge jump at chron 16, insufficient to explain the missing crust. *Cande and Haxby* [1991] proposed repeated small rift jumps occurred at the Adventure trough.

Chron 8. Between chrons 10 and 8, the Chile ridge rotated ~50° clockwise (cw) from striking roughly east-west to ~N40°W (Figures 5c and 6), as evidenced by a change in strike of magnetic isochrons on the ANT plate.

Chron 6C. Chron 6C was a time of major plate boundary reorganizations in the southeast Pacific. There was a roughly 5° ccw change in spreading direction along the PAC-ANT ridge (Figure 6, chron 8 through 6(o)). Along the Chile ridge between chrons 8 and 6(o) there was a ~38° cw rotation of the ridge axis from striking ~N40°W to ~N1°W (Figure 6, chrons 8 and 6(o), respectively). There was also a change in spreading direction along the PAC-NAZ ridge [*Handschumacher,* 1976; *Weissel et al.,* 1977]. Evidence for PAC-NAZ ridge rotation was previously observed by charting Seasat lineations in roughly 20 Ma crust, between 20°S and 25°S, 130°W and 124°W [*Okal and Cazenave,* 1985]. We find the PAC-NAZ ridge rotated roughly 10° cw, from striking N15°W to N5°W (Figure 6, chrons 8 and 6(o), respectively).

By chron 6C, the PAC-ANT-NAZ triple junction had migrated to the latitude of the Chiloe FZ (Figures 5d and 6, chron 6C), as indicated by a continuous sequence of anomalies from chron 6C to the Chile ridge axis between the Chiloe and Guafo FZs. Prior to chron 6C, when the FAR plate was moving with a large northward component relative to ANT (Figures 5b and 5c, insets), the PAC-ANT-FAR triple junction could be expected to migrate northward relative to ANT. By chron 6C, when the Chile ridge was spreading nearly east-west, stable triple junction evolution no longer predicts the observed northward triple junction migration (Figures 5e-5h, insets). There are insufficient data to determine how the triple junction migrated north to the latitude of the Chiloe FZ. Migration by microplate formation and extinction, as proposed above for the Juan Fernandez microplate and observed at chrons 6(o) and 5A, is possible. While the data are too sparse to confirm this possibility, transferred lithosphere associated with this speculative microplate is presented (Figures 5c and 6).

Along the PAC-FAR ridge at chron 6C, apparently along the Mocha transform (one transform north of Agassiz), a ridge propagated northward. The Selkirk trough on the NAZ plate is a pseudofault from this propagation event. There is a gap in the anomaly sequence across the Selkirk trough indicating missing Nazca plate crust. At chron 6(o) the northwest end of the Selkirk trough reconstructs to the eastern edge of the region of transferred lithosphere identified by *Mammerickx* [1992] (at ~103°W, 37°S, in Figure 5d). The reconstruction suggests that this region of transferred lithosphere preserved on the PAC plate (northernmost shaded area, Figure 6, C6(o)) was transferred from the NAZ plate to the PAC plate by the propagation event which formed the Selkirk trough (pseudofault.) This propagation event initiated at chron 6C and was nearly complete by chron 6(o) [*Tebbens et al.,* this issue, Figure 7a]. In this case only the propagating ridge continued spreading; a failed ridge was also identified by *Mammerickx* [1992] nearby on the PAC plate. Stepwise triple junction migration did not occur during this reorganization, probably because of the long along-ridge distance between the triple junction and the propagator (Figure 6, C6(o)).

Chron 6AA. At chron 6AA, the ridge which formed the Selkirk trough (pseudofault) was still propagating and transferring lithosphere from the NAZ plate to the PAC plate. Owing to the large changes in plate spreading directions, no velocity triangles were constructed for the PAC-ANT-NAZ triple junction for the interval from chron 6C to 6(o).

Chron 6(o). At chron 6(o), south of the Valdivia FZ system, a plate boundary reorganization resulted in a migration of the PAC-ANT-NAZ triple junction from the latitude of the Chiloe FZ to the latitude of the Valdivia FZ system. At chron 6(o) the newly charted troughs A and B reconstruct as adjacent features located just south of the Agassiz FZ (Figure 6, C6(o)). The data associated with this reorganization are sparse. The magnetics data indicate a second ridge axis began spreading between the Agassiz and Chiloe FZs, where formerly there had been only PAC-NAZ (FAR) spreading. If the second ridge formed to the east of the PAC-NAZ ridge, troughs A and B may record a decrease in spreading rate and change in spreading direction on the flanks of the southernmost section of PAC-NAZ ridge, while a new ridge began spreading farther east in crust formed previously at the PAC-NAZ ridge. Alternatively, if the second ridge initiated west of the PAC-NAZ ridge, troughs A and B may be the flanks of a fault which separated, with an initiation of seafloor spreading in between. Both proposed evolutions result in a change from one ridge axis to two between the Agassiz and Chiloe FZs (southernmost PAC-NAZ ridge). The two ridges were "captured" as the northernmost segments of the PAC-ANT and Chile ridges. If the stepwise triple junction model [*Tebbens et al.,* this issue] applies, prior to their "capture," during plate boundary reorganization, these ridges were probably spreading independently of the major ridge axes and adding crust to a short-lived microplate. This microplate is east of trough B (transferred lithosphere portion of microplate shown with shading in Figures 5 and 6). The chron 6(o) reorganization resulted in a northward migration of the

PAC-ANT-NAZ triple junction from west of the Chiloe FZ to the Agassiz-Agassiz' FZ (Figure 6, C6(o) to C5C). Either process, with a second ridge axis initiating east or west of the PAC-FAR ridge, is similar to the proposed evolution of the Juan Fernandez microplate (Figure 1) in that a second spreading center formed which "overlapped" the southernmost PAC-NAZ ridge, no ridge failed, and there was transferal of lithosphere to the ANT plate.

Chron 5C. Between chrons 5D (17 Ma) and 5B (15 Ma), there was a slight counterclockwise (ccw) rotation along the Chile ridge which is indicated by a change in strike of the FZs (Plate 1) and magnetic isochrons [*Tebbens et al.*, this issue]. This ccw rotation put the transforms of the Chile ridge under extension. The northernmost transform (Agassiz-Agassiz') was the longest Chile ridge transform (800 km) and connected the Chile ridge to the PAC-ANT-NAZ triple junction. Under extension, the Agassiz-Agassiz' transform separated at chron 5C and seafloor spreading initiated the formation of the Valdivia FZ system. The Valdivia FZ system is now composed of six closely spaced FZs offsetting short (22-27 km in length) ridge segments [*Tebbens et al.*, this issue]. The ANT and NAZ sides of the separated Agassiz-Agassiz' transform are recorded as a pair of WNW trending tectonic discontinuities bounding the Valdivia FZ system (Plate 1).

Chron 5A to chron 5(o). Between chrons 5C and 5(o), near the end of chron 5A (middle Miocene, 12.5 Ma), there was a major reorganization in the southeast Pacific. This reorganization resulted in a stepwise triple junction migration, similar to that outlined for the Juan Fernandez microplate above (Figure 1) and discussed by *Tebbens et al.* [this issue]. Magnetic anomaly data indicate that ridge propagation began at roughly chron 5AD (~14.7 Ma) along the transform which connected the Valdivia FZ system to the PAC-ANT-NAZ triple junction and continued until shortly before chron 5(o), when the propagating ridge reached the Challenger FZ [*Tebbens et al.*, this issue]. The pseudofaults of this propagation event are the Friday and Crusoe troughs (Figure 6, C5A), which are observed as continuous lows in the gravity field (Plate 1) and discontinuities in the magnetic anomaly sequence [*Tebbens et al.*, this issue]. Between chron 5AD and chron 5(o), during propagation, the lithosphere located between the actively propagating ridge, and the overlapped ridge was the Friday microplate [*Tebbens et al.*, this issue]. The propagating ridge transferred crust from the NAZ plate to the short-lived Friday microplate [*Tebbens et al.*, this issue].

The formation and extinction of the Friday microplate resulted in stepwise triple junction migration by a sequence of events similar to those presented for the Juan Fernandez microplate (Figure 1). The ridge axis which comprised the western Friday microplate boundary was the southernmost PAC-NAZ ridge prior to ridge propagation and the northernmost PAC-ANT ridge segment after propagation. The ridge axis which comprised the eastern boundary of the Friday microplate, the propagating ridge, became the northernmost segment of the Chile ridge, between the Valdivia and Chile FZ systems. Thus the east and west microplate ridges were "captured" by the Chile and PAC-ANT ridges, respectively. This evolution resulted in a 500 km northward migration of the PAC-ANT-NAZ triple junction from a position along the southern boundary of the microplate, west of the Valdivia FZ system along the Agassiz FZ (Figure 6, C5C), to the northern boundary of the microplate, along the Chile transform (Figure 6, C5(o)).

The northward migration of the PAC-ANT-NAZ triple junction north of the Valdivia FZ system was previously proposed to have occurred at chron 6C [*Handschumacher*, 1976; *Weissel et al.*, 1977]. Owing to insufficient data, the details of the tectonic evolution were not resolved. Additional data indicate two propagation events north of the Valdivia FZ system, at chrons 6C and 5A (Figures 5 and 6). A propagation event beginning at chron 6C formed the Selkirk trough pseudofault on the NAZ plate but did not result in stepwise triple junction migration. A propagation event beginning at chron 5A formed the Friday and Crusoe trough pseudofaults and resulted in triple junction migration from the Valdivia FZ system to the Chile FZ [*Tebbens et al.*, this issue]. Thus triple junction migration occurred 12 Myr later than proposed by *Weissel et al.* [1977] and *Handschumacher* [1976] and the stepwise migration process is now apparent.

Chron 3B to chron 3. At chron 3A (~5.5 Ma) there was a minor plate reorganization in the southeast Pacific, including significant changes in spreading rates along the PAC-ANT ridge [*Cande and Kent*, 1992], Chile ridge [*Tebbens et al.*, this issue], and EPR [*Lonsdale*, 1989a]. Propagation events along the PAC-ANT ridge produced a nearly linear 1800 km ridge segment [*Lonsdale*, 1994]. At chron 3(o) the Juan Fernandez microplate began to form near the PAC-ANT-NAZ triple junction [*Larson et al.*, 1992]. The evolution of the Juan Fernandez microplate is discussed above.

Chron 3 to Present. Between chron 3 and the Present, spreading continued along the major southeast Pacific ridge axes with no major reorganizations. The Juan Fernandez microplate evolved to its present configuration [*Larson et al.*, 1992] (Figure 6, Present).

Relation to Plate Boundary Reorganizations Throughout the Pacific Basin

The chron 6C propagation event (which formed the Selkirk trough) was synchronous with a major plate boundary reorganization throughout the Pacific. In the eastern Pacific basin, spreading initiated along the Galapagos spreading center, fragmenting the FAR plate into the NAZ plate and Guadeloupe plate [*Handschumacher*, 1976; *Hey et al.*, 1977; *Lonsdale and Klitgord*, 1978; *Mammerickx and Klitgord*, 1982; *Atwater*, 1989].

The chron 5A southeast Pacific reorganization was synchronous with a prolonged interval of reorganization in the northern Pacific. Chron 5A was the time of fragmentation of the Guadeloupe plate into the Cocos and Rivera plates [*Atwater*, 1989; *Lonsdale*, 1991]. At chron 5A, spreading ceased along the ridge segment just north of the Shirley FZ along the Pacific-Guadeloupe ridge and quite possibly ceased along the entire length of ridge west of Baja California [*Mammerickx and Klitgord*, 1982; *Atwater*, 1989; *Lonsdale*, 1991]. South of the Clarion FZ, the Pacific-Guadeloupe spreading center changed spreading direction and became the Pacific-Cocos spreading center. The Mathematician microplate formed and became extinct (effectively a ridge jump) between the "Unnamed" FZ and Galapagos FZ [*Mammerickx and Klitgord*, 1982].

The chron 3A (~5.5 Ma) plate reorganization was also synchronous with an extended interval of plate boundary reorganizations in the northeast Pacific. The EPR propagated northward toward the continental proto-Gulf of California, reaching it around chron 2A(o) (3.55 Ma) [*Lonsdale*, 1989a, Figure 8].

Conclusions

We observe three major plate boundary reorganizations in the southeast Pacific between the late Oligocene and Present, at chrons 6C, 6(o), and 5A, and a minor reorganization at chron 3(o). Each of these reorganizations included ridge axis propagation. The chron 6(o) and chron 5A propagation events transferred crust to the ANT plate, resulting in the northward migration of the PAC-ANT-NAZ triple junction. A model of repeated mid-ocean triple junction migration is proposed which involves ridge axis propagation, microplate formation, and microplate extinction. Evidence for the model is a trail of regions of transferred lithosphere observed along the path of the PAC-ANT-NAZ triple junction which are interpreted as portions of extinct microplates.

Acknowledgments. This work was initiated as part of the first author's dissertation when both authors were at Lamont-Doherty Geological Observatory of Columbia University. This paper greatly benefited from discussions with and/or critical reviews by T. Atwater, W. Haxby, M. Kleinrock, M. Kuykendall, D. Naar, W. Pitman, H Schouten, M. Tivey, and D. Wilson. Figure 5 was drafted by A. M. Alvarez and digitally redrafted by C. Edmisten. This research was supported by the National Science Foundation grant OCE-89-18612 and a University of South Florida President's Council Faculty Award.

References

Atwater, T., Plate tectonic history of the northeast Pacific and western North America, in *The Geology of North America, vol. N, The Eastern Pacific Ocean and Hawaii*, edited by E.L. Winterer et al., pp. 21-72, Geol. Soc. of Am., Boulder, Colo., 1989.

Bird, R. T., and D. F. Naar, Intratransform origins of mid-ocean microplates, *Geology, 22,* 987-990, 1994.

Cande, S. C., and W. F. Haxby, Eocene propagating rifts in the southwest Pacific and their conjugate features on the Nazca plate, *J. Geophys. Res., 96,* 19609-19622, 1991.

Cande, S. C., and D. V. Kent, A new geomagnetic polarity time scale for the late Cretaceous and Cenozoic, *J. Geophys. Res., 97,* 13917-13951, 1992.

Cande, S. C., and D. V. Kent, Revised calibration of the geomagnetic timescale for the Late Cretaceous and Cenozoic, *J. Geophys. Res., 100,* 6093-6095, 1995.

Cande, S. C., E. M. Herron, and B. R. Hall, The early Cenozoic tectonic history of the southeast Pacific, *Earth Planet. Sci. Lett., 89,* 63-74, 1982.

Cande, S. C., J. L. LaBrecque, R. L. Larson, W. C. Pitman III, X. Golovchenko, and W. F. Haxby, Magnetic lineations of the world's ocean basins, Am. Assoc. of Pet. Geol., Tulsa, Okla., 1989.

Cande, S. C., C. A. Raymond, J. Stock, and W. F. Haxby, Geophysics of the Pitman fracture zone and Pacific-Antarctic plate motions during the Cenozoic, *Science, 270,* 947-953, 1995.

Carbotte, S., S. M. Welch and K. C. Macdonald, Spreading rates, rift propagation, and fracture zone offset histories during the past 5 my on the Mid-Atlantic Ridge; 25–27°30' S and 31–34°30'S, *Mar. Geophys. Res., 13,* 51-80, 1991.

Chang, T., On the statistical properties of estimated rotations, *J. Geophys. Res., 92,* 6319-6329, 1987.

Chang, T., Estimating the relative rotation of two tectonic plates from boundary crossings, *J. Am. Stat. Assoc., 83,* 1178-1183, 1988.

Chang, T., J. Stock, and P. Molnar, The rotation group in plate tectonics and the representation of uncertainties of plate reconstructions, *Geophys. J. Int., 101,* 649-661, 1990.

DeMets, C., R. G. Gordon, D. F. Argus, and S. Stein, Current plate motions, *Geophys. J. Int., 101,* 425-478, 1990.

Engeln, J. F., S. Stein, J. Werner, and R. G. Gordon, Microplate and shear zone models for oceanic spreading center reorganizations, *J. Geophys. Res., 93,* 2839-2856, 1988.

Goodwillie, A. M., and B. Parsons, Placing bounds on lithospheric deformation in the central Pacific Ocean, *Earth Planet. Sci. Lett., 111,* 123-139, 1992.

Handschumacher, D. W., Post-Eocene plate tectonics of the eastern Pacific, in *The Geophysics of the Pacific Ocean Basin and Its Margin, Geophys. Monogr. Ser.* , vol. 19, edited by G. H. Sutton et al., pp. 177-202, AGU, Washington, D.C., 1976.

Hellinger, S. J., The uncertainties of finite rotations in plate tectonics, *J. Geophys. Res., 86,* 9312-9318, 1981.

Herron, E. M., Crustal plates and sea-floor spreading in the southeastern Pacific, in *Antarctic Oceanology I, Antarct. Res. Ser.*, edited by J.L. Reid, vol. 15, pp. 229-237, AGU, Washington, D.C., 1971.

Herron, E. M., Sea-floor spreading and the Cenozoic history of the east-central Pacific, *Geol. Soc. Am. Bull., 83,* 1671-1692, 1972.

Hey, R., G. L. Johnson, and A. Lowrie, Recent tectonic evolution of the Galapagos area and plate motions in the East Pacific, *Geol. Soc. Am. Bull., 88,* 1385-1403, 1977.

Hey, R. N., F. K. Duennebier, and W. J. Morgan, Propagating rifts on midocean ridges, *J. Geophys. Res., 85,* 3647-3658, 1980.

Hey, R. N., D. F. Naar, M. C. Kleinrock, J. P. Morgan, E. Morales, and J.-G. Schilling, Microplate tectonics along a superfast seafloor spreading system near Easter Island, *Nature, 317,* 320-325, 1985.

Larson, R. L., R. C. Searle, M. C. Kleinrock, H. Schouten, R. T. Bird, D. F. Naar, R. I. Rusby, E. E. Hooft, and H. Lasthiotakis, Roller-bearing tectonic evolution of the Juan Fernandez microplate, *Nature, 356,* 571-576, 1992.

Lonsdale, P., Geology and tectonic history of the Gulf of California, in *The Geology of North America,* vol. N, *The Eastern Pacific Ocean and Hawaii*, edited by E.L. Winterer et al., pp. 499-521, Geol. Soc. of Am., Boulder, Colo., 1989a.

Lonsdale, P., Segmentation of the Pacific-Nazca spreading center, 1°N -- 20°S, *J. Geophys. Res., 94,* 12197-12225, 1989b.

Lonsdale, P., Structural patterns of the Pacific floor offshore of Peninsular California, in *The Gulf and Peninsular Province of the Californias*, edited by J.P. Dauphin et al., AAPG *Mem., 47,* pp. 87-125, 1991.

Lonsdale, P., Geomorphology and structural segmentation of the crest of the southern (Pacific-Antarctic) East Pacific Rise, *J. Geophys. Res., 99,* 4683-4702, 1994.

Lonsdale, P., and K. D. Klitgord, Structure and tectonic history of the eastern Panama basin, *Geol. Soc. Am. Bull., 89,* 981-999, 1978.

Macdonald, K. C., D. S. Scheirer, and S. M. Carbotte, Mid-ocean ridges: Discontinuities, segments and giant cracks, *Science, 253,* 986-994, 1991.

Mammerickx, J., The Foundation Seamounts: Tectonic setting of a newly discovered seamount chain in the South Pacific, *Earth Planet. Sci. Lett., 113,* 293-306, 1992.

Mammerickx, J., and K. D. Klitgord, Northern East Pacific rise: Evolution from 25 m.y.B.P. to the Present, *J. Geophys. Res., 87,* 6751-6759, 1982.

Mammerickx, J., D. F. Naar, and R. L. Tyce, The Mathematician paleoplate, *J. Geophys. Res., 93,* 3025-3040, 1988.

Mayes, C. L., L. A. Lawver, and D. T. Sandwell, Tectonic history and new isochron chart of the South Pacific, *J. Geophys. Res., 95,* 8543-8567, 1990.

McKenzie, D. P., and W. J. Morgan, Evolution of triple junctions, *Nature, 224,* 125-133, 1969.

Minster, J. B., and T. H. Jordan, Present-day plate motions, *J. Geophys. Res., 83,* 5331-5354, 1978.

Molnar, P., T. Atwater, J. Mammerickx, and S. Smith, Magnetic anomalies, bathymetry and the tectonic evolution of the South Pacific since the late Cretaceous, *Geophys. J.R. Astron. Soc., 40,* 383-420, 1975.

Morgan, W., P. R. Vogt, and D. F. Falls, Magnetic anomalies and sea floor spreading on the Chile rise, *Nature, 222,* 137, 1969.

Naar, D. F., Microplates, in *Encyclopedia of Earth System Science,* vol. 3, pp. 231-237, Academic, San Diego, Calif., 1992.

Naar, D. F., and R. N. Hey, Tectonic evolution of the Easter microplate, *J. Geophys. Res., 96,* 7961-7993, 1991.

Okal, E. A., and A. Cazenave, A model for the plate tectonic evolution of the east-central Pacific based on Seasat investigations, *Earth Planet. Sci. Lett., 72,* 99-116, 1985.

Pardo-Casas, F., and P. Molnar, Relative motion for the Nazca (Farallon) and South America plates since late Cretaceous time, *Tectonics, 6,* 233-248, 1987.

Patriat, P., and V. Courtillot, On the stability of triple junctions and its relation to episodicity in spreading, *Tectonics, 3,* 317-332, 1984.

Pitman, W. C., and J. R. Heirtzler, Magnetic anomalies over the Pacific-Antarctic ridge, *Science, 154,* 1164-1171, 1966.

Royer, J.-Y., and T. Chang, Evidence for relative motions between the Indian and Australian plates during the last 20 m.y. from plate

tectonic reconstructions: Implications for the deformation of the Indo-Australian plate, *J. Geophys. Res., 96,* 11779-11802, 1991.

Rusby, R. I., and R. C. Searle, A history of the Easter microplate, 5.25 Ma to Present, *J. Geophys. Res., 100,* 12617-12640, 1995.

Sandwell, D., Global marine gravity grid and poster developed, *EOS Trans. AGU, 74,* 35, 1993.

Sandwell, D. T., and W. H. F. Smith, Exploring the ocean basins with satellite altimeter data, www.ngdc.noaa.gov/mgg, Natl. Geophys. Data Cent., Boulder, Colo., 1995.

Schouten, H., K. D. Klitgord, and D. G. Gallo, Edge-driven microplate kinematics, *J. Geophys. Res., 98,* 6689-6701, 1993.

Searle, R. C., R. I. Rusby, J. Engeln, R. N. Hey, J. Zukin, P. M. Hunter, T. P. LeBas, H.-J. Hoffman, and R. Livermore, Comprehensive sonar imaging of the Easter microplate, *Nature, 341,* 701-705, 1989.

Searle, R. C., R. T. Bird, R. I. Rusby, and D. F. Naar, The development of two oceanic microplates: Easter and Juan Fernandez microplates, East Pacific rise, *J. Geol. Society London, 150,* 965-976, 1993.

Tebbens, S. F., Tectonic evolution of the southeast Pacific from Oligocene to Present, Ph.D. thesis, Columbia Univ., New York, 1994.

Tebbens, S. F., S. C. Cande, L. Kovacs, J. C. Parra, J. L. Labrecque, and H. Vergara, The Chile ridge: A tectonic framework, *J. Geophys. Res.,* this issue.

Weissel, J. K., D. E. Hayes, and E. M. Herron, Plate tectonic synthesis: The displacements between Australia, New Zealand and Antarctica since the late Cretaceous, *Mar. Geol., 25,* 231-277, 1977.

Wessel, P., and W. H. F. Smith, Free software helps map and display data, *EOS Trans. AGU, 72,* 441, 1991.

S.C. Cande, Scripps Institution of Oceanography, MS 0215, La Jolla, CA 92093. (e-mail: cande@gauss.ucsd.edu)

S.F. Tebbens, Department of Marine Sciences, University of South Florida, St. Petersburg Campus, 140 Seventh Avenue South, St. Petersburg, FL 33701-5016. (e-mail: tebbens@marine.usf.edu)

(Received December 5, 1994; revised June 18, 1996;
accepted August 20, 1996.)